BOCA
BOLETIM DE CONJUNTURA

ELECTRIC-FURNACE PRODUCTION OF ELEMENTAL PHOSPHORUS AND THERMAL PHOSPHORIC ACID: FUNDAMENTALS, THERMODYNAMICS, INDUSTRIAL PRACTICE, DECARBONIZATION, AND FUTURE ROUTES—A CRITICAL REVIEW

PRODUÇÃO DE FÓSFORO ELEMENTAR E ÁCIDO FOSFÓRICO TÉRMICO EM FORNO ELÉTRICO: FUNDAMENTOS, TERMODINÂMICA, PRÁTICA INDUSTRIAL, DESCARBONIZAÇÃO E ROTAS FUTURAS—UMA REVISÃO CRÍTICA

PRODUCCIÓN DE FÓSFORO ELEMENTAL Y ÁCIDO FOSFÓRICO TÉRMICO EN HORNO ELÉCTRICO: FUNDAMENTOS, TERMODINÁMICA, PRÁCTICA INDUSTRIAL, DESCARBONIZACIÓN Y RUTAS FUTURAS—UNA REVISIÓN CRÍTICA

https://doi.org/10.56238/bocav25n82-011

Data de submissão: 02/08/2026 **Data de publicação:** 16/09/2026

Antonio Clareti Pereira[1]

ABSTRACT

The electric-furnace route to elemental phosphorus and thermal phosphoric acid occupies an unusual position in the phosphorus value chain: it is one of the most energy- and carbon-intensive established chemical-metallurgical processes, yet it remains strategically relevant when elemental P_4 or exceptionally low-impurity phosphoric acid is required. This critical review evaluates the route as an integrated system comprising reaction, furnace, gas handling, separation, safety, and product purification rather than as an isolated carbothermic reduction step. A structured critical-narrative corpus of 107 unique in-scope scientific and technical sources was organized around phosphate mineralogy and burden preparation; thermodynamics and kinetics; submerged-arc furnace behavior; product and by-product quality; energy and emissions; competition with purified wet-process phosphoric acid; circularity; and emerging alternatives. Representative industrial evidence indicates electricity use of approximately 13–15 MWh per tonne of P_4, phosphorus recovery of about 85–94%, and slag generation of roughly 8–9 t per tonne of P_4, illustrating the scale of the route's structural resource burden. The synthesis shows that performance is governed by coupled constraints: silica must destabilize calcium phosphate without creating an excessively viscous slag; carbon must provide reduction potential and suitable electrical/physical behavior without excessive fossil-carbon exposure; furnace power must sustain a hot, permeable reaction zone while avoiding unstable electrical operation; and phosphorus vapor must be safely removed, condensed, and purified without transferring unacceptable burdens to tail gas, dust, slag, or wastewater. The conventional route retains a defensible niche where

[1] PhD in Chemical Engineering. Institution: University of São Paulo (USP). E-mail: claretipereira@gmail.com
Orcid: https://orcid.org/0000-0001-8115-4279

the value of P_4 or high-purity thermal acid offsets its electricity- and reductant-intensity. However, purified wet-process acid increasingly erodes the historical purity premium, while carbon pricing and decarbonization targets amplify structural disadvantages. Near-term priorities are burden engineering, phosphorus-specific furnace control, heat and CO-rich-gas recovery, cleaner electricity, and systematic valorization of slag and dust; longer-term options include molten-salt electrolysis, silicothermic reduction, plasma-assisted processing, and recovery from secondary phosphorus resources. A decision framework is proposed linking product specification, electricity carbon intensity, feed quality, impurity tolerance, co-product value, evidence maturity, and technology readiness to route selection.

Keywords: Phosphoric Acid. Elemental Phosphorus. Electric Furnace. Carbothermic Reduction. Phosphate Rock. Decarbonization.

RESUMO

A rota de forno elétrico para fósforo elementar e ácido fosfórico térmico ocupa uma posição inusitada na cadeia de valor do fósforo: é um dos processos químico-metalúrgicos estabelecidos mais intensivos em energia e carbono, contudo permanece estrategicamente relevante quando fósforo elementar P_4 ou ácido fosfórico de excepcional pureza é requerido. Esta revisão crítica avalia a rota como um sistema integrado compreendendo reação, forno, manipulação de gases, separação, segurança e purificação de produtos, em vez de como uma etapa isolada de redução carbotérmica. Um corpus narrativo-crítico estruturado de 107 fontes científicas e técnicas únicas relevantes foi organizado em torno de mineralogia fosfática e preparação da carga; termodinâmica e cinética; comportamento do forno de arco submerso; qualidade de produtos e subprodutos; energia e emissões; competição com ácido fosfórico purificado de processo úmido; circularidade; e alternativas emergentes. Evidência industrial representativa indica uso de eletricidade de aproximadamente 13–15 MWh por tonelada de P_4, recuperação de fósforo de cerca de 85–94%, e geração de escória de aproximadamente 8–9 t por tonelada de P_4, ilustrando a escala do ônus de recurso estrutural da rota. A síntese demonstra que o desempenho é governado por restrições acopladas: sílica deve desestabilizar fosfato de cálcio sem criar uma escória excessivamente viscosa; carbono deve fornecer potencial de redução e comportamento elétrico/físico adequado sem exposição excessiva a carbono fóssil; potência do forno deve sustentar uma zona de reação quente e permeável enquanto evita operação elétrica instável; e vapor de fósforo deve ser removido com segurança, condensado e purificado sem transferir ônus inaceitáveis para gás de cauda, pó, escória ou água residual. A rota convencional retém um nicho defensável onde o valor de P_4 ou ácido térmico de alta pureza compensa sua intensidade em eletricidade e redutores. Contudo, ácido de processo úmido purificado erosiona cada vez mais o prêmio histórico de pureza, enquanto precificação de carbono e metas de descarbonização amplificam desvantagens estruturais. Prioridades de curto prazo são engenharia de carga, controle de forno específico para fósforo, recuperação de calor e gás rico em CO, eletricidade mais limpa e valorização sistemática de escória e pó; opções de longo prazo incluem eletrólise em sal fundido, redução silicotérmica, processamento assistido por plasma e recuperação de recursos secundários de fósforo. Um marco de decisão é proposto vinculando especificação de produto, intensidade de carbono da eletricidade, qualidade da alimentação, tolerância a impurezas, valor de coproduto, maturidade de evidência e prontidão tecnológica à seleção de rota.

Palavras-chave: Ácido Fosfórico. Fósforo Elementar. Forno Elétrico. Redução Carbotérmica. Minério Fosfático. Descarbonização.

RESUMEN

La ruta de horno eléctrico para fósforo elemental y ácido fosfórico térmico ocupa una posición inusual en la cadena de valor del fósforo: es uno de los procesos químico-metalúrgicos establecidos más intensivos en energía y carbono, sin embargo sigue siendo estratégicamente relevante cuando se requiere fósforo elemental P_4 o ácido fosfórico de excepcional pureza. Esta revisión crítica evalúa la ruta como un sistema integrado que comprende reacción, horno, manejo de gases, separación, seguridad y purificación de productos, en lugar de como una etapa aislada de reducción carbotérmica. Un corpus narrativo-crítico estructurado de 107 fuentes científicas y técnicas únicas en el alcance fue organizado alrededor de mineralogía fosfática y preparación de carga; termodinámica y cinética; comportamiento del horno de arco sumergido; calidad de productos y subproductos; energía y emisiones; competencia con ácido fosfórico purificado de proceso húmedo; circularidad; y alternativas emergentes. La evidencia industrial representativa indica un uso de electricidad de aproximadamente 13–15 MWh por tonelada de P_4, recuperación de fósforo de aproximadamente 85–94%, y generación de escoria de aproximadamente 8–9 t por tonelada de P_4, ilustrando la magnitud de la carga de recursos estructurales de la ruta. La síntesis muestra que el desempeño está gobernado por restricciones acopladas: la sílice debe desestabilizar el fosfato de calcio sin crear una escoria excesivamente viscosa; el carbono debe proporcionar potencial de reducción y comportamiento eléctrico/físico adecuado sin exposición excesiva a carbono fósil; la potencia del horno debe mantener una zona de reacción caliente y permeable mientras se evita una operación eléctrica inestable; y el vapor de fósforo debe ser removido de forma segura, condensado y purificado sin transferir cargas inaceptables al gas de cola, polvo, escoria o aguas residuales. La ruta convencional retiene un nicho defendible donde el valor de P_4 o ácido térmico de alta pureza compensa su intensidad en electricidad y reductores. Sin embargo, el ácido de proceso húmedo purificado erosiona cada vez más la prima histórica de pureza, mientras que la fijación de precios del carbono y los objetivos de descarbonización amplifican las desventajas estructurales. Las prioridades a corto plazo son la ingeniería de carga, el control de horno específico para fósforo, la recuperación de calor y gas rico en CO, electricidad más limpia y la valorización sistemática de escoria y polvo; las opciones a largo plazo incluyen electrólisis en sal fundida, reducción silicotérmica, procesamiento asistido por plasma y recuperación de recursos secundarios de fósforo. Se propone un marco de decisión que vincula la especificación del producto, la intensidad de carbono de la electricidad, la calidad de la alimentación, la tolerancia a impurezas, el valor del coproducto, la madurez de la evidencia y la preparación tecnológica a la selección de la ruta.

Palabras clave: Ácido Fosfórico. Fósforo Elemental. Horno Eléctrico. Reducción Carbotérmica. Mineral de Fosfato. Descarbonización.

1 INTRODUCTION

1.1 STRATEGIC IMPORTANCE OF PHOSPHORIC ACID AND ELEMENTAL PHOSPHORUS

Phosphoric acid is a platform chemical whose dominant mass-market use is fertilizer manufacturing, but its strategic importance extends far beyond fertilizer-grade material. Purified acid is required for food ingredients, surface treatment, specialty phosphates, electronics, and, increasingly, battery-related value chains. Elemental phosphorus occupies an even narrower but chemically distinctive position because it is the precursor to organophosphorus compounds, high-purity phosphorus derivatives, and several synthesis pathways that cannot be reproduced simply by concentrating wet-process acid. The electric-furnace route therefore serves two partially overlapping markets: direct production of elemental P_4 and production of thermal phosphoric acid by oxidation and hydration of condensed P_4. Contemporary reviews of phosphorus use, recycling, and thermal technology emphasize both the continuing utility of elemental phosphorus and the growing pressure to redesign how it is made (Duan *et al.*, 2022; Geeson & Cummins, 2020; Gilmour, 2019; Jupp *et al.*, 2021; M. Li *et al.*, 2024; Wingate *et al.*, 2023).

The strategic problem is not whether the electric-furnace route can make high-quality product—it can—but whether its purity and feed-flexibility advantages are sufficient to justify the combination of very high electrical demand, carbonaceous reductant consumption, complex hot-gas handling, and multiple impurity pathways. That question has become more acute as wet-process phosphoric acid purification has advanced and as phosphorus-sector decarbonization has moved from an environmental aspiration to an industrial constraint. Recent systems-level analyses call for phosphorus production routes to be compared in terms of energy, carbon, resource efficiency, and circularity rather than on product purity alone (Bertau *et al.*, 2025; F. Wu *et al.*, 2022; Yao *et al.*, 2024; X. Yu *et al.*, 2026).

1.2 ROUTE COMPETITION AND HISTORICAL EVOLUTION

Historically, the furnace route provided a direct path from phosphate rock to elemental phosphorus and, after controlled oxidation and hydration, to very pure phosphoric acid. Industrial development accelerated after the Second World War as phosphorus derivatives and phosphate detergents expanded, whereas higher electricity prices and restrictions on

phosphate detergents contributed to contraction in several Western markets from the 1970s onward (Gilmour, 2019). The technology nevertheless matured into large, closed, continuously operated electric furnaces with integrated off-gas collection and phosphorus condensation. In this sense, the modern evolution of the route is less a change in the core reaction than a progression from scale-up and electrical stabilization toward improved gas cleaning, energy recovery, digital control, residue valorization, and decarbonization (Gilmour, 2019; M. Li *et al.*, 2024; Yao *et al.*, 2024).

Wet-process technology became dominant for bulk fertilizer acid production because sulfuric acid digestion is less electricity-intensive and avoids reducing phosphate to the elemental state before reoxidizing it. The modern competitive landscape is therefore asymmetric: wet-process acid dominates tonnage, whereas furnace-derived production is justified mainly by the value of elemental P_4, stringent impurity specifications, or downstream chemistry. At the same time, increasingly capable wet-acid purification blurs the historical boundary between fertilizer-grade wet acid and high-purity thermal acid (Becker, 1989; Bertau *et al.*, 2025). The central industrial question is therefore not whether the electric furnace can make a high-quality product—it can—but which functions of the route remain intrinsically valuable and which can be displaced by purification or alternative reduction chemistry. This review consequently treats the thermal route as an integrated value chain whose relevance depends on product slate, electricity source, raw-material impurity pattern, by-product outlets, process safety, and regulatory context rather than on furnace efficiency alone (Geeson & Cummins, 2020; Jupp *et al.*, 2021; Yao *et al.*, 2024; X. Yu *et al.*, 2026).

1.3 OBJECTIVES AND CRITICAL QUESTIONS

The review has five objectives. First, it reconstructs the chemistry and physical logic of carbothermic phosphate reduction, emphasizing how silica, carbon, slag structure, gas removal, and impurity reduction interact. Second, it evaluates submerged-arc furnace operation as an electro-thermo-chemical system, including industrial operating windows, electrical behavior, burden permeability, tapping, and safety-critical gas handling. Third, it follows phosphorus and key impurities through P_4 condensation, thermal-acid production, ferrophosphorus, slag, dust, tail gas, and wastewater. Fourth, it compares the furnace route with modern purified wet-process acid on technical, environmental, and economic grounds

using a common-product/common-boundary logic wherever the evidence permits. Fifth, it identifies realistic improvement pathways and distinguishes near-term optimization of existing assets from longer-term alternatives, such as electrolysis, silicothermic reduction, plasma processing, and secondary resource recovery. The resulting critical question is not “Is the furnace route obsolete?” but “Under which combinations of product value, power carbon intensity, feed composition, impurity tolerance, safety requirements, and circularity does it remain the rational choice?”

2 REVIEW METHODOLOGY AND EVIDENCE BASE

2.1 SCOPE AND CORPUS CONSTRUCTION

The review focused on thermal phosphoric acid, electric-furnace phosphorus, elemental phosphorus production, furnace phosphoric acid, purified wet-process acid, and emerging phosphorus-recovery routes. Scopus, Web of Science, OneMine, Google Scholar, and patent databases were identified as search environments in the bibliographic dossier. The supplied bibliography contained 110 entries. Two entries were exact duplicates of previously listed submerged-arc-furnace and cooling-hydration studies, and one entry concerned persistent organic pollutant emissions from primary copper smelting rather than phosphorus production. These three records were excluded, leaving 107 unique in-scope references. The final corpus is dominated by literature from 2020–August 2026, supplemented by foundational sources required to describe established wet-process and elemental-phosphorus technology.

The original search-stage logs do not provide the initial number of database hits, date-by-date exports, or numerical reasons for exclusion at each screening stage. Those values were therefore not reconstructed retrospectively. Accordingly, this article does not claim a reproducible Preferred Reporting Items for Systematic Reviews and Meta-Analyses (PRISMA) systematic review. It uses a structured critical-narrative protocol: transparent topic definition, bibliographic cleaning, thematic classification, cross-comparison of evidence, explicit evidence weighting, and separation between established industrial practice, phosphorus-specific experimental/modeling evidence, transferable cross-sector evidence, and emerging concepts.

2.2 THEMATIC CODING AND CRITICAL SYNTHESIS

Each source was assigned to one or more evidence domains: (i) raw materials and ore preparation; (ii) thermodynamics, kinetics, and reduction mechanisms; (iii) submerged-arc furnace electrical and transport behavior; (iv) elemental phosphorus, acid production, ferrophosphorus, slag, dust, gas treatment, and process safety; (v) energy, carbon, environmental performance, and digital control; (vi) wet-process purification and route competition; (vii) circular phosphorus recovery; and (viii) emerging electrochemical, silicothermic, plasma, and alternative-reductant routes. Cross-sector submerged-arc-furnace studies were retained only when they contribute transferable evidence on burden distribution, electromagnetic losses, current distribution, heat transfer, or furnace control.

Critical weighting used a five-level evidence hierarchy: Level A included modern industrial phosphorus-furnace data; Level B involved phosphorus-specific pilot/experimental studies; Level C comprised thermodynamic, kinetic, computational, or mechanistic studies; Level D included transferable evidence from similar high-temperature reactors; and Level E covered reviews, conceptual assessments, and early proposals. Greater emphasis was placed on relevance to phosphorus, industrial similarity, transparent data, mechanistic content, and process decision usefulness. A common limitation is the prevalence of mechanistic and laboratory evidence over transparent plant-level cost and mass data. Consequently, economic conclusions focus on cost structure and sensitivity rather than universal production costs, and environmental conclusions avoid a single carbon footprint value across diverse electricity mixes, ore grades, and configurations.

2.3 SEARCH TRANSPARENCY, VERIFICATION PASS, AND LIMITATIONS

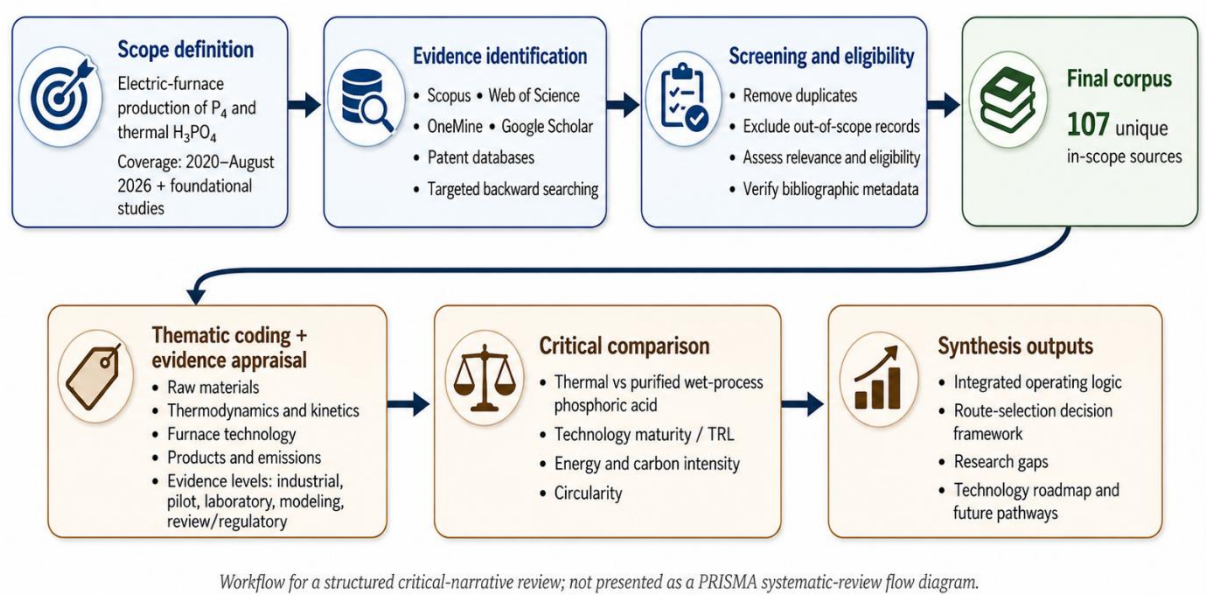
To improve auditability without inventing missing historical search counts, a supplementary verification pass was completed on 23 August 2026 using five Boolean concept blocks: (1) (“elemental phosphorus” OR “yellow phosphorus” OR “thermal phosphoric acid”) AND (“electric furnace” OR carbotherm* OR “submerged arc furnace”); (2) (“phosphate rock” OR phosphorite) AND (thermodynamic* OR kinetic* OR reduction OR slag OR viscosity OR “SiO_2/CaO”); (3) (“yellow phosphorus” OR “thermal phosphoric acid”) AND (energy OR electricity OR carbon OR emission* OR “tail gas” OR purification); (4) (“wet-process phosphoric acid” AND purification) OR (“phosphoric acid” AND “solvent extraction”)

OR nanofiltration OR crystallization; and (5) phosphorus AND ("molten salt electrolysis" OR silicothermic OR plasma OR "sewage sludge" OR "steelmaking slag"). The verification pass was used to confirm quantitative values and bibliographic details of studies already represented in the corpus rather than to create a new systematic-review denominator.

Patent databases are part of the technology-scanning environment but are not used as primary evidence in scientific synthesis. When industrial benchmarks are reported, the manuscript labels them as representative, maintaining source-specific system boundaries. This is important for variables like electricity consumption, carbon footprint, slag generation, and route economics, which vary with feed grade, electricity mix, plant age, and co-products.

Figure 1

Structured critical-narrative review workflow



Workflow for a structured critical-narrative review; not presented as a PRISMA systematic-review flow diagram.

The original search-stage counts were unavailable; the cleaned final corpus contains 107 unique in-scope references.

Source: Author's synthesis of the structured critical-narrative workflow.

3 FEED MATERIALS, BURDEN PREPARATION, AND PROCESS CHEMISTRY

3.1 PHOSPHATE MINERALOGY AND IMPURITY CONSTRAINTS

Commercial furnace feeds are not chemically equivalent even when reported at the same nominal P_2O_5 grade. Apatite-group minerals may contain fluorine and substantial substitutions, while sedimentary collophane can carry iron-, aluminum-, magnesium-, and silica-bearing gangue in forms that affect both reduction chemistry and slag behavior. Work

on mid- and low-grade phosphate ores shows that sesquioxide occurrence, mineral association, particle size, and feed granulometry alter reactivity and the distribution of impurities among slag, ferrophosphorus, dust, and condensed phosphorus. Consequently, ore qualification for a furnace route should be based on mineralogy and impurity deportment—not only bulk P_2O_5 assay (J. Deng *et al.*, 2020; X. Li *et al.*, 2021; Nezamaev *et al.*, 2025).

Pelletizing and agglomeration are process variables rather than merely feed-handling steps. A stable burden must provide sufficient mechanical strength for charging while preserving voidage and gas permeability as solids heat, soften, and react. Recent studies on oxidation-roasted and phosphate-ore pellets indicate continued interest in improving consolidation and burden behavior, consistent with the broader submerged-arc-furnace principle that particle-size distribution and spatial segregation control both electrical resistance and gas flow (Cen *et al.*, 2026; D. He *et al.*, 2025).

3.2 FUNCTIONAL ROLES OF SILICA AND CARBON

Silica is introduced primarily to change the chemical potential of calcium and promote transfer of CaO-equivalent material from phosphate into a silicate-rich slag. The idealized stoichiometry is often represented by the net reaction $2\ Ca_3(PO_4)_2 + 6\ SiO_2 + 10\ C \rightarrow P_4(g) + 6\ CaSiO_3(l) + 10\ CO(g)$. This equation is useful for material-balance thinking but should not be interpreted as a single elementary step. Actual reduction proceeds through evolving solid and liquid phases, local carbon contact, gas generation, and impurity reactions. Experimental work shows that SiO_2 addition, alkali-containing additives, fluxes, and alternative fluxing residues can materially change conversion, slag activation, and reaction kinetics (Z. Chen *et al.*, 2020; Jing *et al.*, 2021; Jing *et al.*, 2025; Long *et al.*, 2024; Luo *et al.*, 2021; G. Zheng *et al.*, 2020).

Carbon simultaneously supplies reduction potential, influences electrical resistivity, creates reactive interfaces, and generates the CO-rich gas stream. Its performance is therefore governed by more than fixed-carbon content. Carbon type, porosity, reactivity, ash chemistry, particle size, and physical contact with phosphate-bearing material affect the observed rate. Vacuum-carbothermal studies and comparisons of carbon sources are

especially useful for separating chemical limitations from gas-phase inhibition and mass-transfer effects (X. He & Huang, 2022; P. Li *et al.*, 2021; Q. Wu *et al.*, 2021).

3.3 LOW-GRADE FEEDS AND PROCESS INTENSIFICATION

The economic attraction of using lower-grade phosphate rock is counterbalanced by higher slag production, greater impurity load, and more difficult burden control. Response-surface optimization, isothermal characterization, and kinetic studies collectively show that acceptable phosphorus release from lower-grade feeds requires coordinated control of temperature, particle size, carbon addition, silica ratio, and residence time rather than a single "optimal" reagent ratio (P. Li *et al.*, 2021; X. Li *et al.*, 2021; Luo *et al.*, 2020; B. Yang *et al.*, 2025). Alternative fluxes and co-reduction concepts—such as fly ash, sulfate residues, or metallurgical slags—can reduce virgin flux demand or recover secondary values, but they also introduce new alkalis, iron, sulfur, or trace-metal pathways that must be evaluated at full-stream level (B. Li *et al.*, 2022; Luo *et al.*, 2021; Tian *et al.*, 2025). High-temperature fouling studies in the SiO_2–CaO–P_2O_5 system further show that phosphate-bearing melts can impose deposition constraints on thermal equipment, reinforcing the need to link feed chemistry to downstream operability (P. Wu *et al.*, 2020).

Table 1 organizes the principal feed components and shows why burden design must be treated as a multi-objective problem rather than a stoichiometric recipe.

Table 1

Functions and critical control variables of major furnace-feed components

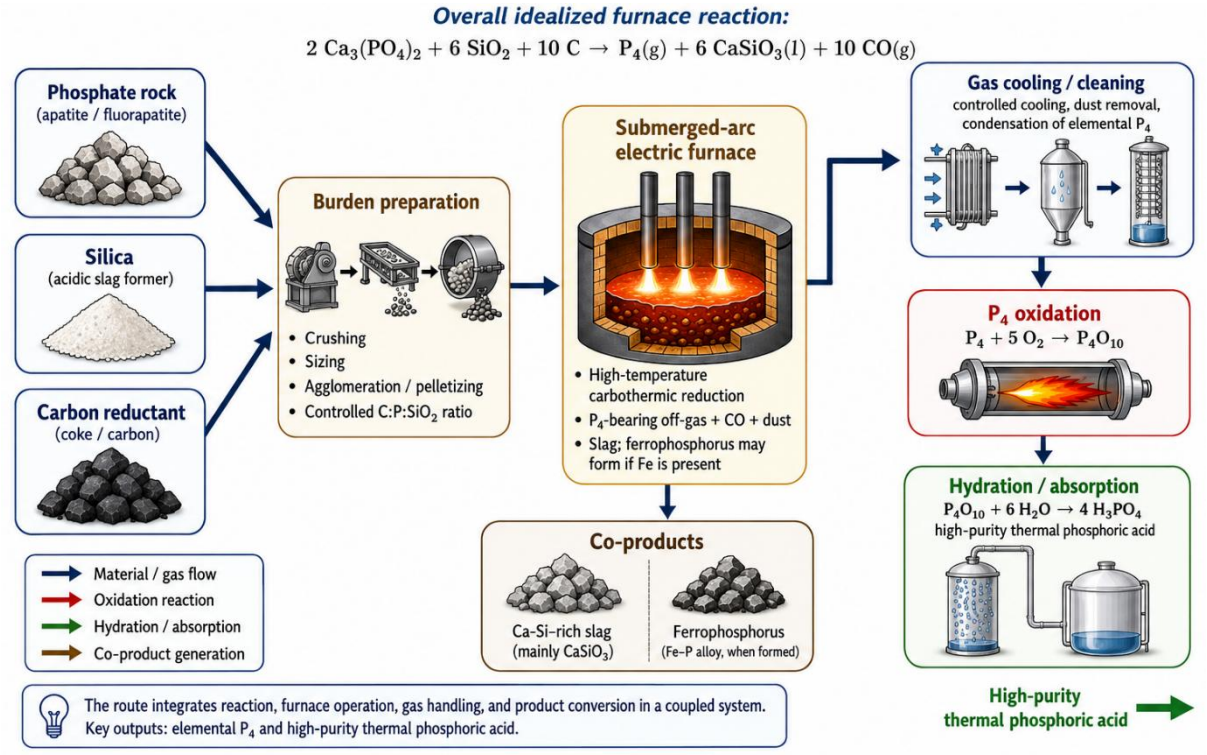
Feed component	Primary function	Critical variables	Principal risk if poorly controlled
Phosphate rock	Phosphorus source	P mineralogy; P_2O_5 grade; Fe/Al/Mg; F; particle size; moisture	Low reactivity, excessive slag, impurity transfer, unstable burden
Silica / siliceous flux	Bind CaO-equivalent material in silicate slag and lower phosphate stability	SiO_2/CaO balance; mineral form; softening behavior	High viscosity or excessive slag volume; altered refractory/electrical behavior
Carbonaceous reductant	Reduce phosphorus oxides and participate in furnace electrical/thermal behavior	Fixed C; reactivity; porosity; ash; size; resistivity	Incomplete reduction, excess carbon use, poor permeability, higher fossil-carbon intensity
Binders/pellet additives	Improve agglomerate strength and size distribution	Dosage; green strength; thermal decomposition; introduced impurities	Fines generation, permeability loss, unwanted fluxing or impurity loading
Secondary fluxes / residues	Potentially replace flux or recover embedded values	Composition consistency; sulfur/metal content; melting behavior	Cross-contamination, volatile emissions, uncertain slag quality

Source: Author's synthesis based on Cen *et al.* (2026), Z. Chen *et al.* (2020), J. Deng *et al.* (2020), D. He *et al.* (2025), X. Li *et al.* (2021), Luo *et al.* (2021), and Tian *et al.* (2025).

Figure 2 places these feed functions in the overall route and emphasizes that furnace chemistry, gas condensation, and thermal-acid production are sequentially coupled.

Figure 2

Integrated electric-furnace route from phosphate rock to thermal phosphoric acid



Source: Author's synthesis based on Gilmour (2019), M. Li *et al.* (2024), Z. Zhu *et al.* (2022), and the process relationships synthesized in this review.

4 THERMODYNAMICS, KINETICS, AND REDUCTION MECHANISMS

4.1 THERMODYNAMIC DRIVING FORCE AND GAS-PHASE COUPLING

Phosphate reduction is difficult because calcium phosphate and related apatite phases are thermodynamically stable. The furnace route overcomes this stability by combining high temperature, carbon activity, silica-driven stabilization of calcium in a silicate slag, and continuous removal of volatile phosphorus from the reaction environment. Thermodynamic analyses of electric-furnace and alternative phosphorus routes consistently show that the favorable direction of reaction depends on the coupled chemical potentials of carbon, oxygen, calcium-bearing slag, and gaseous phosphorus species rather than on temperature alone (Khajouei *et al.*, 2025; Long *et al.*, 2024; Z. Zhu *et al.*, 2022).

The gas phase is not a passive product sink. Formation and evacuation of CO and phosphorus-bearing vapor influence local equilibrium and can change the apparent temperature required for release. Vacuum-carbothermal studies are valuable because they demonstrate how lowering gas-phase partial pressures can intensify reduction even when the solid reactants are unchanged (X. He & Huang, 2022; Long *et al.*, 2024). Industrial furnaces cannot simply reproduce laboratory vacuum conditions, but the same principle supports rapid gas disengagement, adequate bed permeability, and avoidance of stagnant zones where product gases can locally suppress forward reaction.

4.2 SLAG CHEMISTRY, VISCOSITY, AND PHOSPHORUS PARTITIONING

The slag is a thermodynamic reagent, a heat-transfer medium, an electrical environment, and a separation phase. Its composition must be sufficiently acidic to stabilize calcium silicate and destabilize phosphate, yet sufficiently fluid to permit mass transfer, gas release, and tapping. Recent measurements of yellow-phosphorus slag show that both P_2O_5 content and the SiO_2/CaO ratio alter melt viscosity and structure, while changes in cation affinity influence phosphorus association, phase separation, and the persistence of residual phosphorus in the slag (Lu *et al.*, 2023; Lu *et al.*, 2024; Lu *et al.*, 2025). These findings explain why increasing silica can improve one aspect of reduction while degrading another through higher slag volume or viscosity.

Iron-bearing phases create an additional sink because reduced phosphorus can alloy with iron to form ferrophosphorus. Simultaneous reduction of P_2O_5- and FeO-bearing slags confirms that phosphorus recovery to the gas phase and phosphorus partitioning to metal are coupled through oxygen potential and metal availability (H. Yu, Miki, *et al.*, 2022). The practical objective is therefore not maximum phosphate reduction in isolation, but maximum recovery of phosphorus to the desired product while controlling Fe–P alloy formation and residual phosphorus in the slag.

4.3 KINETIC LIMITATIONS AND ALTERNATIVE REDUCTANTS

Kinetic studies based on isoconversional analysis and particle-size effects indicate that the controlling regime can shift as reduction proceeds: early solid-state or interfacial reaction may give way to diffusion through product layers, liquid-phase transport, or gas-removal

limitations. This makes a single global activation energy an incomplete descriptor of industrial performance (P. Li *et al.*, 2021; B. Yang *et al.*, 2025). Alternative reductants and briquetted carbon systems are therefore interesting not only because of carbon sourcing but because they may change contact geometry, electrical resistance, and reaction pathway. Anthracite–phosphate–silicon briquettes, for example, illustrate how reductant substitution can be engineered together with burden structure rather than evaluated as a simple coke replacement (Pak *et al.*, 2026).

To move the synthesis from qualitative mechanism to decision-relevant ranges, Table 2 consolidates quantitative benchmarks from phosphorus-specific studies. These values should not be merged into a single universal operating optimum because pressure, feed mineralogy, slag composition, particle size, and experimental scale differ among studies; their value is to define orders of magnitude and interaction windows.

Table 2

Representative quantitative thermodynamic and kinetic benchmarks for carbothermic phosphorus release

Study/condition	Quantitative benchmark	Process interpretation	Evidence level
Z. Zhu et al. (2022), electric-furnace system	Slag acidity $M_k \approx 0.75–0.85$; apparent activation energy 165.712 kJ/mol	Flux chemistry and eutectic formation alter both reaction thermodynamics and kinetics; the apparent kinetics were described as first-order under the study conditions.	C
P. Li et al. (2021), particle-size study	Apparent activation energy decreased from 371.74 to 321.11 kJ/mol as phosphate-rock size decreased from 100–150 to 38–48 μm	Finer feed improved apparent kinetics; the reported behavior was consistent with a shrinking-core formulation.	B/C
Long et al. (2024), vacuum carbothermal reduction	At 1300 °C and SiO_2/CaO = 1.25, phosphorus volatilization reached 91.98%	Silica promoted Ca-silicate formation and mass transfer, but excessive silica impaired reactant–carbon contact and gas diffusion.	B/C
Lu et al. (2023), P_2O_5-bearing slag	At 1380 °C, viscosity increased from 1.00 to 1.82 Pa·s as P_2O_5 increased from 0.7 to 3.9 wt%	Residual P_2O_5 can materially change slag flow above the liquidus temperature and therefore tapping and mass transfer.	B
Lu et al. (2024), SiO_2/CaO series	For 85 wt% (SiO_2 + CaO) and SiO_2/CaO = 0.9, the reported optimal discharge range was 1252–1285 °C; industrial tapping is commonly about 1400–1450 °C	The slag-discharge temperature can potentially be reduced for specific compositions, but only within a composition-specific liquidus/viscosity window.	B

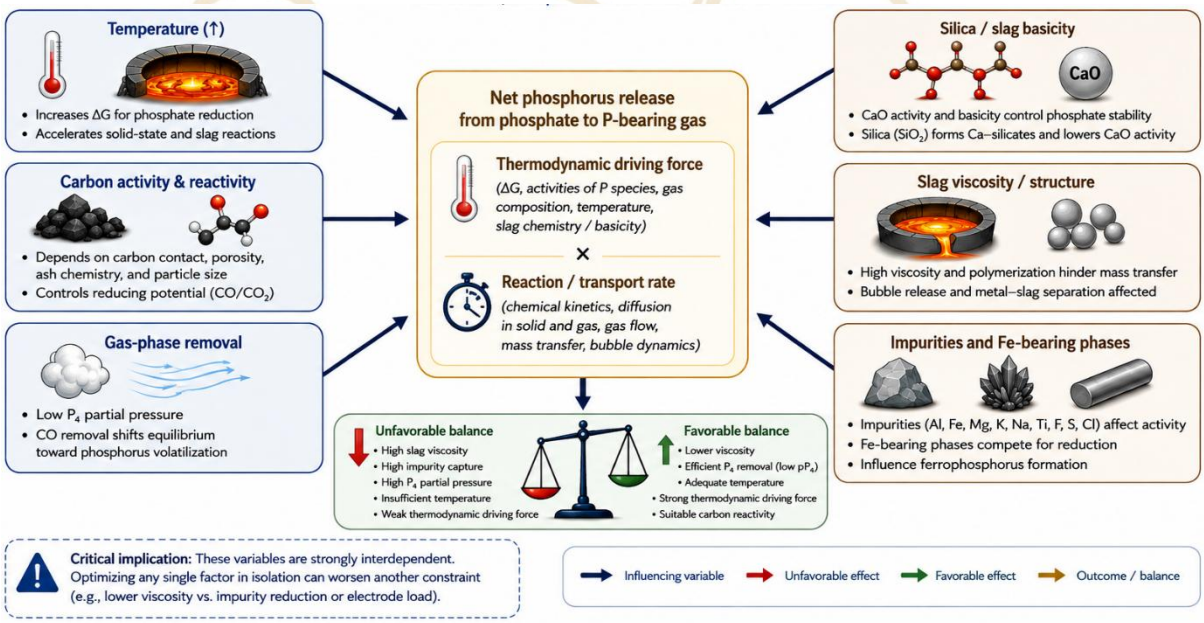
Values are study-specific and are not presented as universal plant set points.
Source: Author's synthesis based on Z. Zhu *et al.* (2022), P. Li *et al.* (2021), Long *et al.* (2024), and Lu *et al.* (2023, 2024).

The quantitative evidence reinforces the central trade-off: conditions that improve phosphate destabilization or phosphorus volatilization can simultaneously alter viscosity, liquid-phase fraction, reactant contact, and gas transport. The industrial control target is therefore an operating window—rather than a single temperature, acidity, or reagent ratio—in which reaction driving force, slag mobility, burden permeability, and phosphorus partitioning remain simultaneously acceptable.

Figure 3 summarizes the principal thermodynamic and kinetic levers and highlights the main critical insight of this section: the process is governed by interacting constraints, so a variable that is favorable in an equilibrium calculation may still be detrimental to furnace hydraulics, slag tapping, impurity partitioning, or electrode performance.

Figure 3

Coupled thermodynamic and kinetic controls on phosphorus release



Source: Author's synthesis based on X. He and Huang (2022), Long *et al.* (2024), Lu *et al.* (2023, 2024, 2025), B. Yang *et al.* (2025), H. Yu, Miki, *et al.* (2022), and Z. Zhu *et al.* (2022).

5 ELECTRIC-FURNACE TECHNOLOGY AND OPERATIONAL CONTROL

5.1 SUBMERGED-ARC FURNACE ARCHITECTURE AND ELECTRICAL BEHAVIOR

The phosphorus furnace belongs to the wider family of submerged-arc and resistance-heated furnaces in which electrode position, burden resistivity, current paths, and local reaction zones determine where electrical energy is dissipated. General ferroalloy practice provides the conceptual foundation, while modern numerical studies show that current distribution is strongly affected by geometry, material properties, and electrode configuration (Gasik *et al.*, 2020; Luckins *et al.*, 2022; Tesfahunegn *et al.*, 2020; Tesfahunegn *et al.*, 2021). Although not all of these studies use phosphorus feeds, their transferable message is directly relevant: electrical efficiency cannot be separated from burden distribution and thermal state.

Discrete-element modeling of submerged-arc-furnace burden distribution demonstrates how segregation and packing influence electrical resistance, while full-scale electromagnetic modeling shows that eddy-current losses and current pathways can be material at large scale (Baumgartner *et al.*, 2024; X. Tang *et al.*, 2026). Cross-sector analyses of direct-current and alternating-current furnaces further reinforce the importance of power distribution and furnace geometry when evaluating energy efficiency (Tesfahunegn *et al.*, 2020; Y. Yu *et al.*, 2023). These tools should be interpreted as enabling models, not as substitutes for phosphorus-specific property data.

5.2 HEAT AND MASS TRANSFER, BURDEN PERMEABILITY, AND REACTION-ZONE STABILITY

A stable furnace requires simultaneous control of solids descent, gas ascent, heat transfer, and liquid drainage. The burden must heat progressively without collapsing into a low-permeability layer before gas evolution can escape. Studies of heat and mass transfer in large submerged-arc and gasification reactors, although not all phosphorus-specific, illustrate how reactor geometry, flow distribution, and localized heat release generate nonuniform operating zones (G.-J. Chen *et al.*, 2026; X. Tang *et al.*, 2025). For phosphorus production, these nonuniformities are especially important because local over-heating can accelerate volatilization and refractory attack, whereas colder or over-compacted regions retain unreduced phosphate and destabilize electrical load.

5.3 TAPPING, OFF-GAS HANDLING, AND FURNACE–DOWNSTREAM INTEGRATION

The furnace has at least three simultaneous product exits: phosphorus-bearing gas, silicate slag, and ferrophosphorus. Their rates are coupled. Delayed slag tapping changes hearth level and electrical conditions; excessive metal accumulation alters current paths and phosphorus losses; and unstable gas generation challenges condensation and tail-gas treatment. The process must therefore be operated as a furnace-plus-gas-train system. Heat-recovery simulations for furnace-process phosphoric acid underline the significance of sensible heat downstream of the furnace, while apparatus development for cooling-hydration service illustrates that downstream thermal and mass-transfer equipment can constrain the performance of the upstream smelting step (Du *et al.*, 2021; Volnenko *et al.*, 2023).

5.4 DIGITALIZATION AND MODEL-ASSISTED CONTROL

Digital-twin and computer-assisted control studies in phosphorus and related apatite-processing systems show a clear trend toward integrating material balances, energy efficiency, process-state estimation, and optimization (Dli *et al.*, 2020; Dli *et al.*, 2021; Meshalkin *et al.*, 2021). More recent three-dimensional computational fluid dynamics (CFD) work on slag reduction in a submerged-arc furnace for phosphorus recovery from sewage sludge demonstrates how reduced-order or computationally inexpensive models may support broader process exploration (Wieser *et al.*, 2026). The opportunity for industry is not a generic artificial-intelligence (AI) furnace, but a physically constrained supervisory layer that reconciles electrode data, power factor, burden additions, off-gas composition, pressure, tap behavior, and product recovery.

Table 3 summarizes the principal manipulated and monitored variables together with representative industrial benchmarks. The numerical ranges are deliberately presented as reference envelopes rather than design guarantees because ore grade, furnace geometry, power system, and product specification vary among plants.

Table 3

Operational variables, failure modes, and representative benchmarks in an electric phosphorus furnace

Variable / response	Operational significance	Failure mode if poorly controlled	Representative benchmark / evidence
Electrode position and current	Controls resistance, local power density, and reaction-zone location	Current instability, hot spots, low conversion, electrode damage	250–350 V average potential between electrodes; power factor 0.96–0.98 for a representative 60-MW furnace (Gilmour, 2019).
Burden size distribution and charging pattern	Controls permeability, segregation, and electrical path	Channeling, bridging, pressure fluctuation, uneven descent	Per tonne P_4: ~8–12 t fluorapatite ore, 1.2–1.7 t coke, and 1–2.5 t silica in representative large-furnace data (Gilmour, 2019).
Silica/carbon/phosphate ratio	Sets reaction chemistry and slag quantity	Incomplete reduction, excessive slag, high residual P, poor tapping	Composition-specific; silica dosage must be reconciled with slag liquidus/viscosity and carbon contact rather than fixed by stoichiometry alone.
Furnace pressure and off-gas flow	Maintains gas removal and safe containment	P_4 leakage, gas backpressure, unstable condensation	Off-gas ~2.3–2.7 t/t P_4; typical gas temperature ~200–450 °C depending on collection configuration (Gilmour, 2019).
Slag temperature/viscosity and tap rate	Controls liquid drainage and phosphorus loss	Frozen tap, hearth accumulation, entrainment, refractory stress	Slag ~8–9 t/t P_4; representative tapping 1400–1600 °C; lower composition-specific discharge windows have been demonstrated experimentally (Gilmour, 2019; Lu et al., 2024).
Ferrophosphorus inventory	Controls metal sink for P and furnace hearth conditions	Excess phosphorus loss to alloy, altered electrical behavior	Ferrophosphorus ~0.03–0.2 t/t P_4 in representative large-furnace data; overall P_4 recovery reported at ~85–94% (Gilmour, 2019).

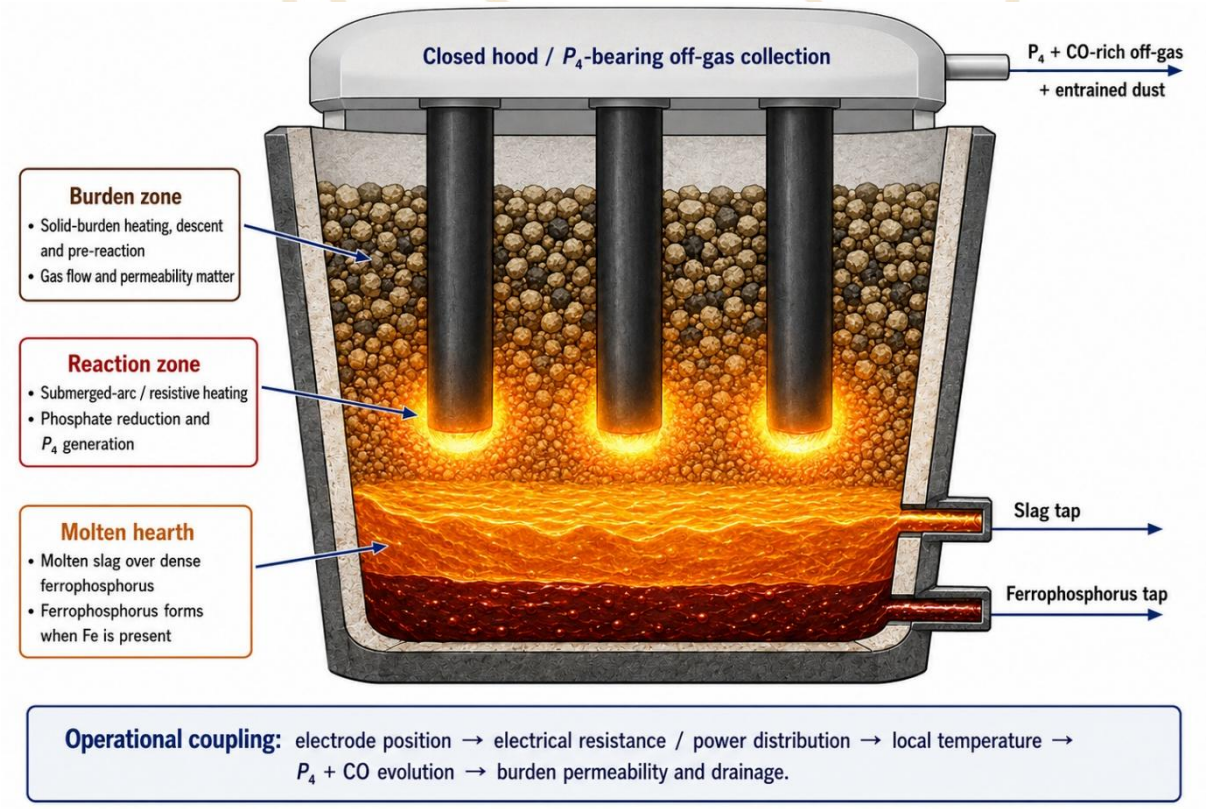
Variable / response	Operational significance	Failure mode if poorly controlled	Representative benchmark / evidence
Specific electrical energy / overall recovery	Defines dominant utility exposure and links furnace stability directly to cost and carbon intensity	High operating cost, high indirect CO_2 burden, reduced throughput if unstable	~13–15 MWh/t P_4 for representative large-furnace operation; 13.051 MWh/t in a 50,000 t/a Chinese case study (Gilmour, 2019; X. Wang et al., 2023).

Source: Author's synthesis based on Gilmour (2019), Gasik *et al.* (2020), Luckins *et al.* (2022), Baumgartner *et al.* (2024), X. Tang *et al.* (2025, 2026), Tesfahunegn *et al.* (2020, 2021), Lu *et al.* (2024), and X. Wang *et al.* (2023).

Figure 4 provides a conceptual section through a closed submerged-arc furnace and indicates the coupling among electrode position, reaction zone, gas evolution, and liquid tapping.

Figure 4

Conceptual submerged-arc furnace for elemental phosphorus production



Source: Author's synthesis based on Gasik *et al.* (2020), Luckins *et al.* (2022), Baumgartner *et al.* (2024), and submerged-arc-furnace modeling concepts reviewed in this article.

6 PRODUCTS, BY-PRODUCTS, IMPURITY PATHWAYS, AND RESOURCE EFFICIENCY

6.1 ELEMENTAL PHOSPHORUS AND THERMAL PHOSPHORIC ACID

The primary volatile product is elemental phosphorus, conventionally recovered by cooling and condensation under conditions designed to minimize uncontrolled oxidation. The condensed P_4 can be sold or oxidized deliberately to phosphorus pentoxide and hydrated to phosphoric acid. This sequence explains the route's purity advantage: many nonvolatile mineral impurities can be rejected before acid formation. However, volatile or semi-volatile impurities can accompany P_4 and require dedicated purification. Vacuum-distillation studies on industrial yellow phosphorus illustrate the importance of arsenic removal, while broader elemental-phosphorus reviews emphasize that purity and safe handling are inseparable because P_4 is highly reactive and requires controlled storage and transfer (Duan *et al.*, 2022; Jiang *et al.*, 2024).

Process safety is a first-order design constraint rather than an ancillary operating issue. Commercial white/yellow phosphorus is highly air-reactive and can ignite spontaneously when exposed to air; industrial condensation, storage, and transfer therefore require reliable exclusion of oxygen, commonly through water-sealed/water-covered or otherwise inerted containment (Gilmour, 2019; Duan *et al.*, 2022). Loss of containment can combine phosphorus fire/burn hazards with toxic or flammable atmospheres from CO-rich gas and trace PH_3, H_2S, HCN, and related species. A defensible plant design consequently couples pressure control, air-ingress prevention, leak detection, reliable condenser seals, controlled phosphorus-water circuits, segregated drainage, and gas purification rather than treating safety as a downstream add-on (Gilmour, 2019; Itkulova *et al.*, 2021; J. Li *et al.*, 2022).

6.2 FERROPHOSPHORUS AND SLAG

Ferrophosphorus is formed when iron-bearing feed constituents are reduced and phosphorus partitions to the metallic phase. Mechanistic work on Fe–P interface migration shows that ferrophosphorus formation is not merely an unavoidable impurity sink; it is a distinct alloying pathway controlled by iron availability, reduction potential, and contact with phosphorus-bearing species (Jing *et al.*, 2024). The product may have value in metallurgical applications, but that value depends on its composition and market access. From a plant

perspective, phosphorus recovered as saleable ferrophosphorus is fundamentally different from phosphorus lost into an off-specification metal phase.

Yellow-phosphorus slag is dominated by calcium–silicate material but may retain phosphorus and trace metals. Reviews and experimental work on slag utilization show opportunities in construction materials, environmental applications, granulated products, and—in carefully controlled compositions—nutrient-related uses (X. Liu *et al.*, 2024; Z. Liu *et al.*, 2023). Flux-modification research further suggests that slag chemistry can be intentionally engineered toward downstream utilization rather than treated as a fixed waste composition (Jing *et al.*, 2025). The critical caveat is that valorization must follow contaminant characterization; a high-volume outlet is not beneficial if it disperses fluoride or trace metals into uncontrolled environments. Studies of phosphorus-production waste formation likewise show that slag and secondary solids must be characterized as evolving process products rather than treated as generic inert waste (Smailov *et al.*, 2024).

6.3 DUST, VOLATILE IMPURITIES, AND TAIL-GAS SPECIES

Dust and gas-treatment residues can concentrate elements that are minor in the ore but economically or environmentally important. Gallium recovery from yellow-phosphorus flue dust demonstrates that a pollution-control residue can also be a secondary metal resource (Ji *et al.*, 2020). Conversely, arsenic in condensed phosphorus and dust requires rigorous segregation and purification (Jiang *et al.*, 2024). Material-flow studies of yellow-phosphorus production and broader assessments of phosphorus-industry by-product links both support a plant-wide accounting approach in which environmental performance is judged by where impurities end up, not only by the concentration in the main product (Dang *et al.*, 2020; F. Wu *et al.*, 2022).

The residual gas after phosphorus condensation is commonly CO-rich but can contain phosphine, sulfur compounds, cyanide-related species depending on feed and process conditions, and fine aerosols. Research on catalytic oxidation of phosphine, electrochemically enhanced liquid-phase purification, Pd/Cu catalytic systems, Rectisol treatment, and methanol absorption of COS/CS_2 shows a diverse technology portfolio for cleaning this stream (Borangazieva *et al.*, 2023; Itkulova *et al.*, 2021; J. Li *et al.*, 2022; Pan *et al.*, 2026; Y. Yang *et al.*, 2025; Y. Yang *et al.*, 2026; Zhao *et al.*, 2023). The most important integration

question is whether the cleaned CO-rich gas can be recovered as fuel or chemical energy rather than flared or diluted, because gas valorization directly affects both energy efficiency and net carbon intensity.

Table 4 summarizes the main product and by-product streams and the process decisions that determine whether each becomes a product, recoverable resource, or liability.

Table 4

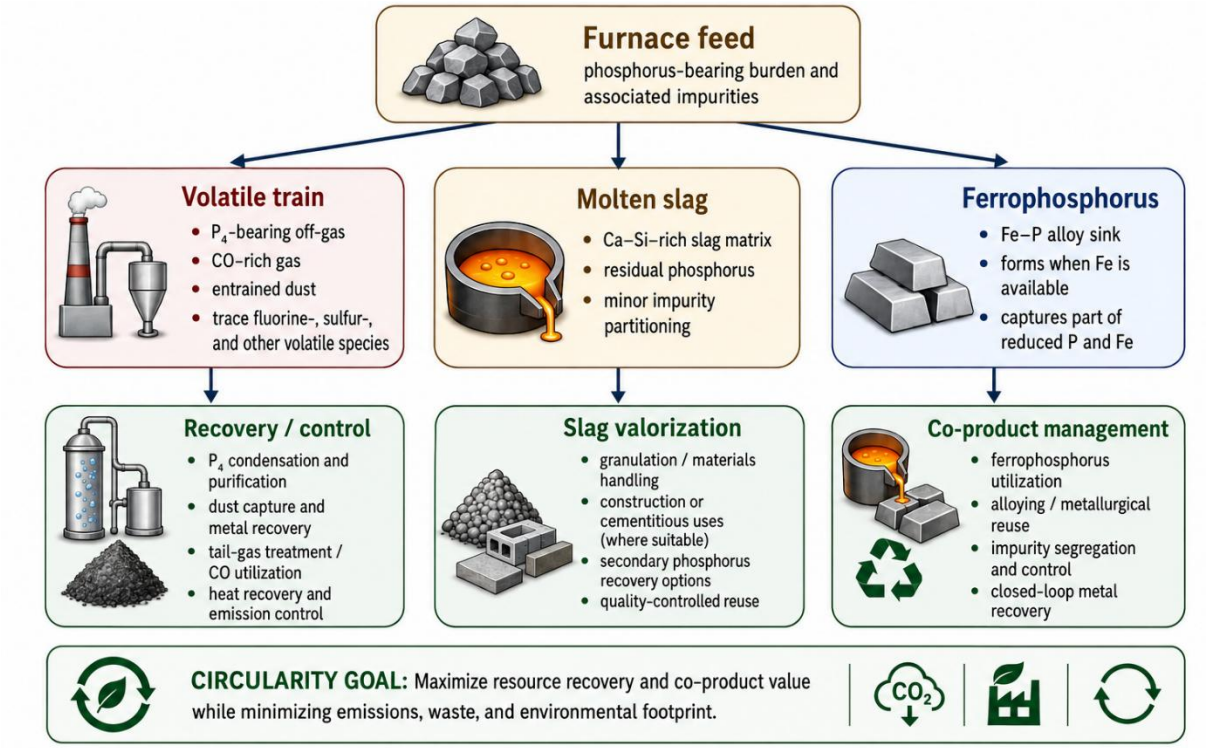
Principal product and by-product streams in furnace phosphoric-acid production

Stream	Dominant constituents/role	Critical quality or fate issue	Potential value/management route
Condensed elemental phosphorus	P_4 with volatile/condensable impurities	As and other volatile impurities; oxidation control; safe storage	Sale as P_4 or feed to thermal H_3PO_4 production
Thermal phosphoric acid	H_3PO_4 formed after controlled P_4 oxidation/hydration	Ultra-low metals and particulate contamination; water quality	High-purity acid for specialty, electronic, food, or chemical use
Ferrophosphorus	Fe–P alloy with reduced metallic impurities	P grade and impurity specification	Metallurgical co-product if marketable
Furnace slag	Ca–Si-rich glass/slag with residual P and trace elements	Residual P, F, metals, leachability, physical form	Granulated aggregate, cementitious/raw material, controlled resource recovery
Flue dust / condensed solids	Fine mineral and volatilized impurity phases	Enrichment of As, Ga, P, F, and other trace species	Selective metal recovery or hazardous-residue management
Tail gas	Predominantly CO after P_4 condensation plus trace contaminants	PH_3, sulfur species, aerosols; calorific value	Purification and energy recovery; avoid uncontrolled combustion/emission

Source: Author's synthesis based on Dang *et al.* (2020), Itkulova *et al.* (2021), Ji *et al.* (2020), Jiang *et al.* (2024), X. Liu *et al.* (2024), and F. Wu *et al.* (2022).

Figure 5

Material-fate architecture and circularity opportunities



Source: Author's synthesis based on Dang *et al.* (2020), Ji *et al.* (2020), X. Liu *et al.* (2024), F. Wu *et al.* (2022), and the integrated stream analysis developed in this review.

7 PROCESS PERFORMANCE, ENERGY INTEGRATION, AND ENVIRONMENTAL BURDEN

7.1 PERFORMANCE METRICS BEYOND PHOSPHORUS CONVERSION

A furnace can achieve high local phosphate conversion and still perform poorly as an industrial process if phosphorus is lost to slag or ferrophosphorus, if electrode or carbon consumption is excessive, or if the gas train limits throughput. Performance should therefore be expressed as a hierarchy of metrics: phosphorus recovery to desired product, specific electrical energy, specific carbon consumption, slag generation per unit phosphorus, phosphorus loss to slag and metal, electrode consumption, off-gas energy recovery, and availability. Representative large-furnace data place specific electricity consumption at approximately 13–15 MWh/t P_4, phosphorus recovery at about 85–94%, slag generation at roughly 8–9 t/t P_4, and ferrophosphorus generation at approximately 0.03–0.2 t/t P_4 (Gilmour, 2019). These values are not universal set points, but they establish the scale against which

incremental efficiency claims should be judged. This multi-metric view is consistent with current assessments of yellow-phosphorus technology under carbon-neutrality constraints and avoids optimizing conversion at the expense of total resource efficiency (Yao *et al.*, 2024).

7.2 ELECTRICITY AND CARBON AS STRUCTURAL CONSTRAINTS

Electricity is not simply a utility cost; it is the dominant route-defining input because the process requires high-temperature reduction and melting. Carbon is similarly structural because the conventional chemistry generates CO as a direct reduction product. A life cycle assessment (LCA) of a 50,000 t/a Chinese yellow-phosphorus plant reported 13,051.27 kWh of electricity per tonne of product and a total carbon footprint of 1.580×10^4 kg CO_2 per tonne, with tail-gas treatment and purchased electricity accounting together for 90.08% of the reported footprint (X. Wang *et al.*, 2023). This single-plant result should not be generalized across grids or furnace configurations, but it quantifies why both the electricity mix and the fate of CO-rich gas dominate decarbonization. Thus, electrification alone does not automatically decarbonize the route: a coal-intensive grid can negate the presumed advantage of electric heating, while renewable electricity reduces indirect emissions but does not eliminate process carbon from carbothermic reduction.

The logical decarbonization sequence is therefore: minimize specific energy through furnace and burden control; source lower-carbon electricity; improve yield so that less input is required per tonne of saleable phosphorus; recover sensible heat; utilize the CO-rich gas; reduce fossil-carbon intensity of the reductant where technically feasible; and, where residual emissions remain material, evaluate carbon capture in the context of gas composition and economics. Industrial-park analyses reinforce that low-carbon transition must be coordinated across utilities, gas networks, by-product use, and plant integration rather than implemented as isolated equipment projects (X. Yu *et al.*, 2026).

7.3 HEAT RECOVERY, TAIL-GAS PURIFICATION, AND DIGITAL EFFICIENCY

Furnace-process phosphoric acid contains multiple recoverable energy streams: hot furnace gas, high-temperature slag, hot phosphorus oxidation products, and purified CO-rich tail gas. Simulation work has specifically examined heat-energy recovery in the furnace-phosphoric-acid process, while experimental slag granulation addresses recovery of sensible

heat and production of a more usable solid product (Du *et al.*, 2021; Z. Liu *et al.*, 2023). These opportunities should be evaluated together because the destination of heat affects gas cleaning, condensation, water balance, and downstream equipment size.

Digitalization can reduce energy intensity indirectly by stabilizing operation and avoiding excursions that generate fines, unstable power, frozen taps, or off-specification products. Energy/resource-efficiency digital twins, intelligent control architectures, and computer-assisted optimization in phosphorus-related systems provide a basis for this approach (Dli *et al.*, 2020; Dli *et al.*, 2021; Meshalkin *et al.*, 2021). Their practical value depends on measurement quality and model maintenance; a poorly reconciled digital model can merely automate inconsistent operating data.

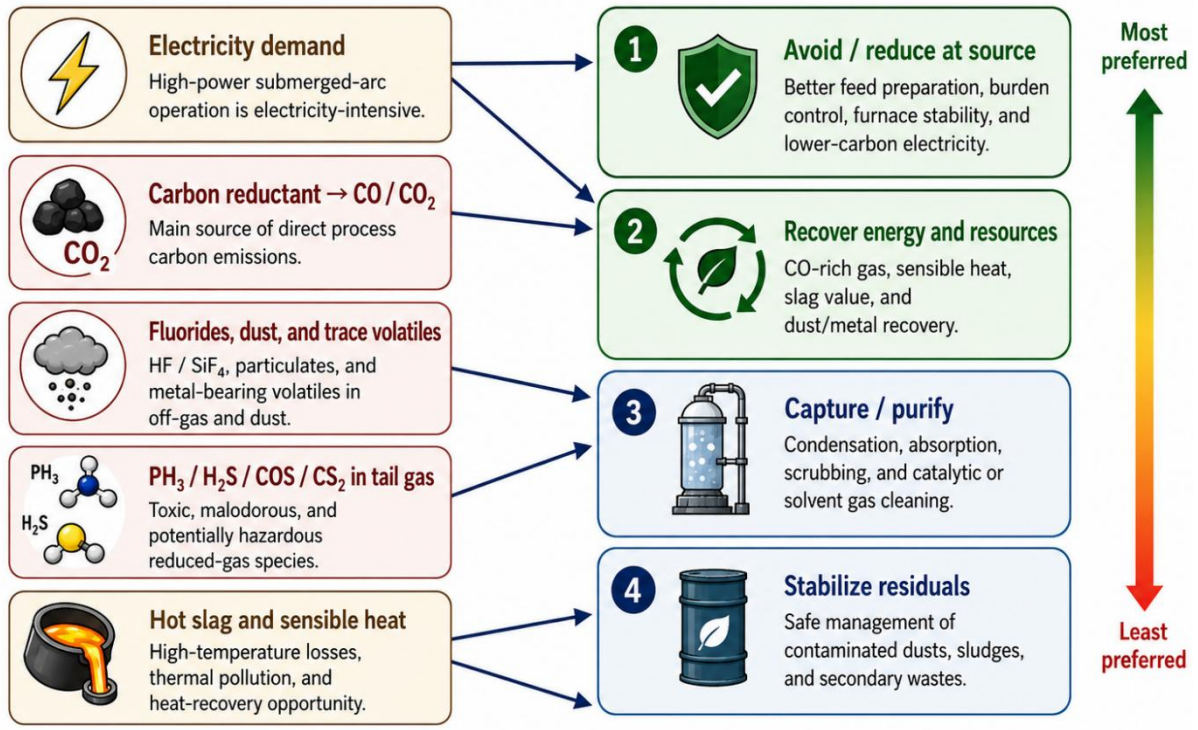
7.4 ENVIRONMENTAL CONTROL HIERARCHY

Environmental control is most effective when emissions are treated as material-fate problems. For gas streams, the preferred sequence is to prevent contaminant formation where possible, condense recoverable phosphorus efficiently, remove toxic trace species with fit-for-purpose purification, and then recover the energy content of the cleaned gas. The recent development of Rectisol-based $PH_3/H_2S/CO_2$ removal, methanol absorption for COS/CS_2, and catalytic phosphine purification demonstrates continued improvement in end-of-pipe capability (Itkulova *et al.*, 2021; Pan *et al.*, 2026; Y. Yang *et al.*, 2025; Y. Yang *et al.*, 2026; Zhao *et al.*, 2023). Yet these technologies do not remove the underlying energy/carbon burden of the furnace itself.

Figure 6 summarizes the resulting environmental control hierarchy and separates decarbonization measures from contaminant-control measures.

Figure 6

Environmental pressure points and preferred control hierarchy



Source: Author's synthesis based on Itkulova *et al.* (2021), X. Wang *et al.* (2023), F. Wu *et al.* (2022), Y. Yang *et al.* (2025, 2026), and Pan *et al.* (2026).

8 COMPETITION WITH WET-PROCESS AND PURIFIED WET-PROCESS PHOSPHORIC ACID

8.1 THE PURITY ADVANTAGE IS REAL BUT NO LONGER ABSOLUTE

The traditional comparison is straightforward: thermal acid is produced from purified elemental phosphorus and therefore contains very low levels of nonvolatile mineral impurities, whereas wet-process acid inherits dissolved metals, fluorine species, suspended solids, organics, and process-specific contaminants from acidulation and gypsum separation. That distinction remains chemically valid, but industrial relevance depends on the attainable purity after modern purification. Reviews and recent studies show rapid progress in precipitation, solvent extraction, nanofiltration, crystallization, and impurity-specific control of wet-process acid (Ali, 2024; Bahsaine *et al.*, 2022; Ding *et al.*, 2025; Gong *et al.*, 2024; Guo *et al.*, 2025; Khaless *et al.*, 2022; J. Wang *et al.*, 2025; C. Xu *et al.*, 2025; C. Xu *et al.*, 2026; S. Xu *et al.*, 2022; L. Yu *et al.*, 2026; R. Zhu *et al.*, 2026).

Impurity management in wet acid is increasingly selective rather than generic. Studies address heavy-metal extraction, multidentate ligands for Fe^{3+}, complexation-precipitation of Mg^{2+}/Al^{3+}, and highly acid-stable nanofiltration membranes. This matters strategically because the furnace route's premium cannot be justified by the statement "wet acid is impure" without defining the target specification and the cost of reaching it. For some electronic or specialty grades, thermal acid may still offer a simpler pathway to purity; for other high-tech grades, a purified wet-process route can increasingly compete.

8.2 GYPSUM, SLUDGE, AND IMPURITY PARTITIONING IN THE WET ROUTE

Wet-process plants exchange the electric furnace's slag and CO-rich gas burdens for large gypsum streams, acid clarification/purification residues, and liquid-phase impurity management. Research on one-step $CaSO_4$ production, clean gypsum routes, co-crystalline phosphorus control, and phosphoric-acid sludge illustrates both the scale of this challenge and the opportunity for higher-value co-products and resource recovery (X. Deng *et al.*, 2026; Fang *et al.*, 2023; Jang *et al.*, 2024; S. Tang *et al.*, 2026). Experimental solid–liquid equilibrium data for phosphate-containing aqueous systems further underline the importance of precipitation chemistry in purified wet-process flowsheets (Z. Zheng *et al.*, 2020).

8.3 ROUTE-SELECTION LOGIC

A rigorous route comparison must normalize to the same saleable product and include upstream reagents, electricity, water, impurity removal, by-product handling, and waste liabilities. Wet-process technology has a decisive advantage for bulk fertilizer acid because it avoids elemental phosphorus production, whereas the thermal route gains value as the required impurity limits tighten or when P_4 itself is required. Feed quality also changes the result: lower-grade phosphate can penalize both routes, but through different mechanisms—higher slag and furnace load in the thermal route versus higher impurity load, gypsum complexity, and purification demand in the wet route. Design-of-experiments work on phosphoric acid process impurities and broader reviews of wet-process technology reinforce the need to base route selection on impurity response rather than on grade alone (Abdelouahhab *et al.*, 2022; Becker, 1989; Ding *et al.*, 2025).

Table 5 compares the two routes on the dimensions that most strongly influence a modern investment decision.

Table 5

Critical comparison of electric-furnace/thermal and wet-process phosphoric-acid routes

Decision dimension	Electric-furnace / thermal route	Wet-process + purification route
Primary chemistry	Reduce phosphate to P_4, condense, oxidize, hydrate	Acidulate phosphate directly; separate gypsum; purify acid as required
Electricity exposure	Very high and structurally important	Lower for acid production; purification can add electricity and reagent demand
Process carbon	Direct carbonaceous reductant demand in conventional route	No carbothermic reduction; indirect emissions from sulfuric acid, utilities, and purification
Intrinsic impurity rejection	Strong for many nonvolatile mineral impurities before acid formation	Impurities enter acid/liquid circuits and must be selectively removed
Major solid stream	Ca–Si-rich furnace slag plus ferrophosphorus/dust	Phosphogypsum plus clarification/purification residues
Best strategic fit	Elemental P_4 and ultra-low-impurity specialty acid where purity premium is high	Bulk fertilizer acid and increasingly high-purity acid when purification is economical
Key decarbonization lever	Low-carbon electricity + lower-carbon reductant + gas/heat recovery	Low-carbon sulfuric acid/utilities + efficient purification + gypsum valorization
Representative quantitative burden	~13–15 MWh electricity/t P_4; ~1.2–1.7 t coke/t P_4; ~8–9 t slag/t P_4; ~85–94% P_4 recovery in representative large-furnace data (Gilmour, 2019).	No single harmonized numerical benchmark was generalized from the corpus because wet-acid purification intensity depends strongly on acid grade, impurity load, purification train, and product specification.
Required normalized comparison basis	Same saleable H_3PO_4 or P_4 specification; include electricity, reductant, gas cleaning, slag/ferrophosphorus/dust management, water, and co-product credits.	Same saleable H_3PO_4 specification; include phosphate beneficiation, H_2SO_4, gypsum handling, water, purification reagents/energy, residues, and co-product credits.

Quantitative comparison is reported only where the corpus provides a defensible common basis.
Source: Author's synthesis based on Becker (1989), Gilmour (2019), Bertau *et al.* (2025), Bahsaine *et al.* (2022), Ding *et al.* (2025), Gong *et al.* (2024), Khaless *et al.* (2022), and C. Xu *et al.* (2025, 2026).

9 TECHNO-ECONOMIC COMPETITIVENESS AND CRITICAL ASSESSMENT

9.1 COST STRUCTURE AND SENSITIVITY

The furnace route is unusually exposed to electricity price because electrical energy is both the principal heat source and a determinant of production rate. Carbon reductant, phosphate rock, silica, electrodes, refractory and maintenance, gas cleaning, phosphorus condensation, oxidation/hydration equipment, and environmental control add to operating expenditure (OPEX) and capital expenditure (CAPEX). Heat-recovery studies indicate that process integration can offset part of this burden, but no recovery scheme removes the fundamental requirement to supply high-temperature reduction energy (Du *et al.*, 2021). The most meaningful sensitivity variables are therefore electricity price and carbon intensity, feed-grade/slag ratio, phosphorus recovery, carbon consumption, plant availability, and the product-value premium for P_4 or high-purity acid. A transparent normalized sensitivity illustrates the scale: at 13.051 MWh/t P_4, every USD 10/MWh change in electricity price changes the electricity-only cost by approximately USD 131/t P_4. Under the 15.8 t CO_2/t P_4 case-study footprint reported by X. Wang *et al.* (2023), each USD 10/t CO_2 carbon price corresponds to roughly USD 158/t P_4 of gross carbon-cost exposure within that specific system boundary. These calculations are illustrative sensitivities, not universal production costs.

Technoeconomic work on phosphoric-acid sludge recovery and thermodynamic/experimental studies of alternative phosphorus production are useful reminders that process economics must include co-product value and avoided disposal, not only main-product yield (Jang *et al.*, 2024; Khajouei *et al.*, 2025). For a furnace plant, saleable ferrophosphorus, useful slag, recovered metals from dust, and utilized CO-rich gas can improve the net cost position. The reverse is also true: if these streams require costly treatment or have no market, the apparent simplicity of a high-purity product is offset by secondary liabilities.

9.2 COMPETITIVE NICHE AND STRATEGIC RISKS

The critical strength of the thermal route is product-function certainty: it can supply elemental phosphorus and can produce phosphoric acid with extremely low concentrations of many mineral-derived impurities. Its weaknesses are structural energy intensity, direct

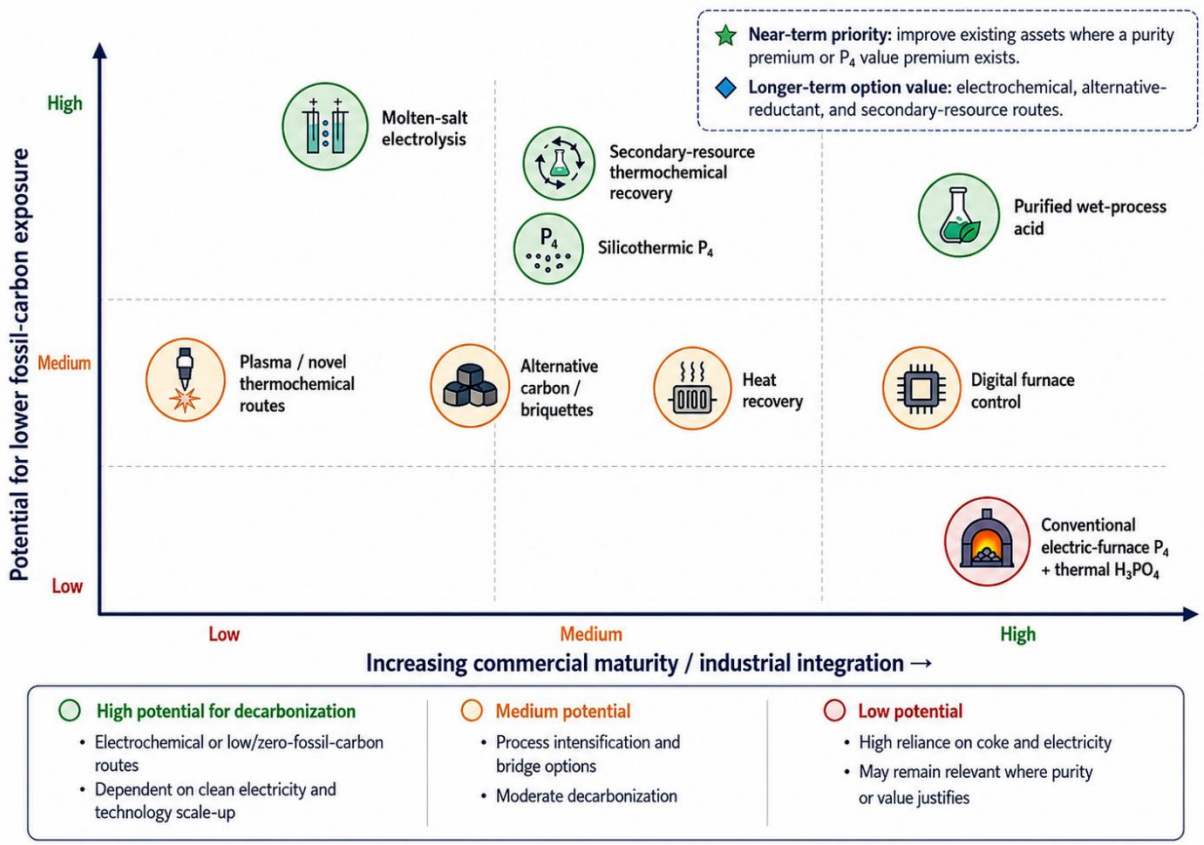
carbon dependence, and complex hazardous-material handling. Its opportunities lie in specialty high-purity markets, low-carbon power regions, high-value co-products, and advanced furnace integration. Its threats are cheaper purified wet-process acid, carbon pricing, restricted access to low-cost electricity, and the maturation of non-carbothermic phosphorus technologies (Bertau *et al.*, 2025; Geeson & Cummins, 2020; M. Li *et al.*, 2024; X. Wang *et al.*, 2023; Yao *et al.*, 2024; X. Yu *et al.*, 2026).

The resulting economic decision is market-specific. A plant producing commodity phosphoric acid without a purity premium is unlikely to justify the thermal route against efficient wet-process production. A plant integrated with downstream organophosphorus chemistry or that requires white/yellow phosphorus may still lack an equivalent wet-process substitute. This distinction is crucial because “thermal acid competitiveness” and “elemental phosphorus competitiveness” are related but not identical investment questions.

Figure 7 qualitatively positions conventional and emerging routes using two explicit ordinal criteria. Commercial maturity is interpreted on a five-level scale from 1 (laboratory concept) to 5 (mature continuous industrial practice). Fossil-carbon exposure is interpreted from 1 (no intrinsic stoichiometric fossil-carbon requirement, assuming low-carbon electricity) to 5 (direct stoichiometric carbon use combined with high electricity-related exposure). The plotted positions represent evidence-weighted strategic screening rather than formal technology-readiness-level (TRL), life-cycle, or cost scores; uncertainty is greatest for early electrochemical, silicothermic, and plasma routes where continuous-operation data remain limited.

Figure 7

Strategic positioning and technology roadmap for phosphorus production



Source: Author's synthesis based on Geeson and Cummins (2020), X. Yang and Nohira (2020), Melville *et al.* (2023), Kashiwakura *et al.* (2025), Bertau *et al.* (2025), and the critical synthesis in this review. Axis positions use the ordinal criteria defined in the text and are not formal TRL or LCA rankings.

10 CIRCULAR ECONOMY AND SECONDARY PHOSPHORUS RESOURCES

10.1 FROM LINEAR PHOSPHATE MINING TO PHOSPHORUS CIRCULATION

The conventional furnace route is historically built around mined phosphate rock, but phosphorus security and waste-management pressures increasingly favor recovery from secondary materials. Material-flow analyses and circularity reviews show that secondary phosphorus appears in sewage sludge and ash, steelmaking slags, biomass-derived ashes, phosphoric-acid residues, and mineral-processing by-products (Abildayeva *et al.*, 2021; Jupp *et al.*, 2021; Lidman Olsson *et al.*, 2023; Wingate *et al.*, 2023; H. Yu, Lu, *et al.*, 2022). These materials differ from phosphate rock in one critical respect: phosphorus concentration is only

one part of the problem; iron, aluminum, silicon, calcium, heavy metals, organics, and halogens often define the technically feasible recovery route.

10.2 THERMOCHEMICAL RECOVERY FROM WASTES AND RESIDUES

Thermochemical studies of sewage sludge demonstrate that phosphorus can be released under inert or reducing conditions and subsequently separated from the gas phase, while complementary thermodynamic evaluations assess the feasibility of recovering elemental phosphorus directly from sludge-derived material (Franke *et al.*, 2025; Franke *et al.*, 2026; Kotze *et al.*, 2025). These studies reconnect secondary-resource recovery with the core furnace principle: phosphorus can be converted into a volatile elemental or gaseous form and then separated, but the impurity inventory of the secondary feed may be more complex than that of beneficiated phosphate rock.

Other circular routes use metallurgical residues as reagents or phosphorus sources. Co-reduction of copper slag with phosphate rock illustrates cross-industry integration, while recovery of phosphorus from steelmaking slag has been reviewed as a potential contribution to sustainable phosphorus supply (B. Li *et al.*, 2022; H. Yu, Lu *et al.*, 2022). Upcycled crude phosphoric acid has also been examined as a feed for carbothermic white-phosphorus production, showing that thermal reduction need not begin with run-of-mine phosphate rock (H. Yu *et al.*, 2024).

10.3 COUPLED RECOVERY OF PHOSPHORUS AND OTHER CRITICAL ELEMENTS

The strongest circular-economy cases are those in which phosphorus recovery is combined with recovery or controlled segregation of other valuable elements. Processes for separating phosphorus and rare earth elements (REEs) from associated phosphate ores, recovering gallium from furnace dust, and recovering elemental phosphorus by electrochemical means from sewage sludge ash demonstrate this principle (Ji *et al.*, 2020; Xie *et al.*, 2024; Zhong *et al.*, 2023). The economic implication is that a secondary-resource route should be judged by the value of the entire recovered product portfolio and the avoided disposal burden, rather than by phosphorus yield alone.

Table 6 summarizes the principal secondary-resource pathways represented in the corpus and the critical scale-up question for each.

Table 6

Secondary phosphorus resources and recovery logic

Secondary resource	Illustrative recovery logic	Potential co-benefit	Critical scale-up question
Sewage sludge / sludge ash	Thermochemical release or electrochemical extraction of elemental phosphorus	Destruction/segregation of organics; ash diversion; possible metal management	Can volatile/metal contaminants be controlled at industrial gas-cleaning scale?
Steelmaking slag	Selective reduction/separation of phosphorus-bearing phases	Improved steel-slag circularity and reduced primary phosphate demand	Can phosphorus be recovered without excessive energy and iron co-reduction?
Phosphoric-acid residues / crude acid	Reprocessing, purification, or carbothermic conversion	Recover P and potentially REEs/metals; avoid sludge disposal	Is impurity concentration an advantage for recovery or a purification liability?
Associated REE phosphate ores	Coordinated separation of P and rare earths	Multiple saleable products	Can a flowsheet avoid transferring P or REE losses between circuits?
Furnace dust	Selective thermal/hydrometallurgical recovery of enriched metals	Recovery of Ga and other concentrated trace values	Are dust volumes and grades sufficient to justify dedicated recovery?

Source: Author's synthesis based on Franke *et al.* (2025, 2026), Ji *et al.* (2020), H. Yu, Lu, *et al.* (2022), H. Yu *et al.* (2024), Xie *et al.* (2024), and Zhong *et al.* (2023).

11 EMERGING TECHNOLOGIES AND FUTURE RESEARCH DIRECTIONS

11.1 MOLTEN-SALT ELECTROLYSIS AND ELECTROCHEMICAL PHOSPHORUS PRODUCTION

Molten-salt electrochemistry is the most conceptually direct attempt to remove fossil carbon from the reduction step: phosphate is dissolved or dispersed in a molten chloride environment and electrochemically reduced to elemental phosphorus. Foundational demonstrations proposed electrolysis of dissolved phosphate in molten chloride, while subsequent studies have examined oxide-deficient melts, electrochemical reduction of PO_4^{3-}, and the dissolution behavior of $Ca_3(PO_4)_2$, $FePO_4$, $Mg_3(PO_4)_2$, $AlPO_4$, and fluorapatite-derived feeds (Y. He & Yang, 2025; G. Liu *et al.*, 2024; G. Liu & X. Yang, 2025; Ma & Yang, 2024; Melville *et al.*, 2023; X. Yang & Nohira, 2020; Y. Yu & Yang, 2024; Zhong & Yang, 2021; Zhong *et al.*, 2022; Zhong *et al.*, 2024).

The attraction is clear: if the anode/cathode chemistry and electricity supply are appropriately designed, electrolysis could decouple phosphorus production from stoichiometric fossil-carbon consumption. The scale-up barriers are equally clear: salt inventory and purification, corrosion-resistant materials, current efficiency, mass transfer of phosphate species, product separation from reactive P_4, electrolyte contamination by gangue, and the cost of high-temperature electrochemical equipment. Electrochemical isolation of phosphorus from sewage-sludge ash expands the concept to secondary resources but also increases impurity complexity (Zhong *et al.*, 2023).

11.2 SILICOTHERMIC AND ALTERNATIVE-REDUCTANT ROUTES

Silicothermic reduction replaces carbon with silicon as the principal reductant and has been proposed as a lower-temperature, by-product-lean route when silicon waste is available. Recent work reports a promising low-temperature pathway using silicon waste, which is strategically interesting because it links phosphorus production to circular use of another energy-intensive material (Kashiwakura *et al.*, 2025). The key systems question is whether the upstream environmental burden of silicon production and the value of silicon waste still yield a lower total footprint than carbothermic reduction. This must be answered with integrated life-cycle and economic analysis rather than reaction temperature alone.

Alternative carbonaceous burdens can offer a nearer-term transition. Anthracite briquettes containing phosphate compounds and silicon illustrate how reductant substitution, briquetting, and reaction promotion can be combined into a single burden-engineering strategy (Pak *et al.*, 2026). Such approaches are more compatible with existing furnace infrastructure than entirely new electrochemical routes, but they still require demonstration of mechanical strength, electrical behavior, impurity transfer, and sustained industrial availability.

11.3 PLASMA AND OTHER HIGH-ENERGY ACTIVATION ROUTES

Plasma processing seeks to intensify phosphate decomposition through highly energetic thermal or reactive environments. Microwave-plasma decomposition of phosphate rock and hydrogen-plasma treatment of phosphorus-bearing mineral systems demonstrate the broader potential of plasma chemistry to alter phosphate stability and volatilization (Ridlo

et al., 2026; H. Zheng *et al.*, 2021). However, plasma should not be automatically described as a low-energy alternative: energy conversion efficiency, torch/electrode lifetime, gas consumption, and heat-transfer scaling can offset kinetic advantages. Its most credible future role may be in concentrated, high-value, or difficult secondary feeds rather than direct replacement of very large conventional furnaces.

11.4 RESEARCH AGENDA AND DECISION FRAMEWORK

The literature suggests six priority research directions. First, thermodynamic databases and kinetic models should be linked to measured high-temperature slag structure and viscosity, so that reduction and tapping can be optimized simultaneously. Second, furnace models should be validated with phosphorus-specific electrical and transport properties rather than borrowed wholesale from ferroalloys. Third, material-fate models should close the fate of phosphorus, fluorine, arsenic, gallium, sulfur, carbon, and iron across gas, slag, metal, dust, and liquid circuits. Fourth, industrial decarbonization studies should explicitly report the electricity mix, reductant origin, gas utilization, and co-product credits. Fifth, emerging electrochemical, silicothermic, and plasma routes should be compared at a common product specification and system boundary. Sixth, purified wet-process acid should be treated as a moving benchmark whose achievable impurity levels and purification cost continue to improve.

Table 7 translates these priorities into decision-relevant research questions, identifies the current level of evidence using the hierarchy defined in Section 2.2, and specifies the minimum evidence required before a new route can credibly displace or complement the electric furnace.

Table 7

Priority research questions for the next generation of phosphorus production

Research question	Why it matters	Minimum evidence needed for decision-making	Current evidence level
Can phosphorus recovery be increased without raising slag viscosity or Fe–P losses?	Directly links yield to furnace operability	Coupled equilibrium/kinetic model + pilot mass balance + slag/metal partition data	B/C
Can existing furnaces use lower-carbon reductants or redesigned briquettes?	Near-term decarbonization with lower retrofit risk	Mechanical, electrical, kinetic, impurity, and long-duration operating data	B/C
Can CO-rich tail gas and sensible heat be fully integrated?	Reduces net energy cost and environmental burden	Site energy integration, gas-cleaning specification, validated heat-recovery balance	A/B
Can purified wet-process acid meet the same end-use specification at lower total cost?	Defines whether the thermal purity premium remains real	Product-specific impurity limits, full purification OPEX/CAPEX, residue management	A/B, but not harmonized
Can molten-salt electrolysis scale beyond laboratory cells?	Potentially removes stoichiometric fossil carbon from reduction	Current efficiency, corrosion lifetime, electrolyte recycle, continuous P_4 separation, technoeconomics	B/C
Can secondary resources support stable large-scale P production?	Links phosphorus security and circular economy	Feed variability envelope, impurity fate, recovery yield, co-product value, regulatory acceptance	B/C

Evidence levels: A = industrial phosphorus data; B = phosphorus-specific pilot/high-temperature experiments; C = phosphorus-specific thermodynamic/kinetic/computational evidence; D = transferable cross-sector evidence; E = review/conceptual evidence.
Source: Author's synthesis based on X. Yang and Nohira (2020), Melville *et al.* (2023), G. Liu *et al.* (2024), G. Liu and X. Yang (2025), Kashiwakura *et al.* (2025), Pak *et al.* (2026), and Bertau *et al.* (2025).

12 CONCLUSIONS

The electric-furnace route to elemental phosphorus and thermal phosphoric acid should be evaluated as an integrated phosphorus-recovery system rather than as an isolated carbothermic reduction reaction. Its overall performance emerges from the interaction among furnace chemistry, electrical behavior, burden permeability, slag properties, gas evolution and removal, phosphorus condensation, process safety, and downstream purification. The route retains a distinctive technical advantage because it can produce elemental P_4 and

exceptionally low-impurity thermal phosphoric acid, but this advantage is accompanied by substantial structural resource requirements. Representative industrial performance indicates electricity consumption of approximately 13–15 MWh per tonne of P_4, phosphorus recovery below that of complete conversion, and the generation of several tonnes of slag per tonne of phosphorus produced. These characteristics make energy efficiency, phosphorus yield, residue management, and co-product utilization central to the long-term viability of the process.

The synthesis further demonstrates that silica dosage, reductant properties, furnace temperature, slag structure, electrical resistance, and phosphorus-gas removal cannot be optimized independently. Industrial performance therefore depends on maintaining an operating window in which thermodynamic driving force, reaction and mass-transfer kinetics, slag viscosity, burden permeability, phosphorus partitioning, tapping stability, electrode behavior, and containment of hazardous species remain simultaneously acceptable. Improvements in one variable may create adverse effects elsewhere in the system, reinforcing the need for integrated process control rather than single-parameter optimization. At the same time, the competitive benchmark for the electric-furnace route has changed. Untreated wet-process phosphoric acid is no longer the appropriate reference because modern precipitation, solvent extraction, membrane separation, crystallization, and related purification technologies increasingly allow wet-process routes to produce high-purity products. Meaningful route comparison must therefore be based on equivalent saleable product specifications and consistent system boundaries that account for electricity, reagents, emissions, residues, purification requirements, and co-product credits.

For existing electric-furnace assets, the most credible near-term opportunities are improved burden engineering, phosphorus-specific model-assisted furnace control, increased phosphorus recovery, cleaner electricity, utilization of CO-rich off-gas, sensible-heat recovery, improved gas-handling and condensation safety, and systematic valorization of slag, dust, and ferrophosphorus. These measures are increasingly relevant not only environmentally but also economically because electricity prices, electricity carbon intensity, and carbon-pricing mechanisms can strongly influence production costs and route competitiveness. Over the longer term, molten-salt electrolysis, silicothermic reduction, plasma-assisted processing, and thermochemical or electrochemical recovery of phosphorus

from secondary resources broaden the technology portfolio and may reduce dependence on conventional coke-based reduction. Their industrial significance, however, will depend on convincing evidence of continuous operation, materials durability, impurity management, phosphorus recovery and purification, energy efficiency, scalability, safety, and whole-system economics. Consequently, no phosphorus-production route should be regarded as intrinsically superior without comparison at a common product specification, transparent assumptions regarding electricity and reductants, consistent environmental and economic boundaries, and evidence commensurate with the claimed level of technological maturity.

DECLARATIONS

Funding: No external funding was reported for this review.

Conflicts of interest: The author declares no known competing financial interests or personal relationships that could have appeared to influence the work reported in this article.

Data availability: No new experimental data were generated. The evidence base consists of the scientific and technical literature cited in the article.

Author contributions: Conceptualization, methodology, literature synthesis, critical analysis, visualization, and writing were performed by the author.

REFERENCES

1. Abdelouahhab, M., Manar, S., & Benhida, R. (2022). Optimization and evaluation of the effect of impurities on phosphoric acid process performance using design of experiments. Results in Engineering, 15, 100501. https://doi.org/10.1016/j.rineng.2022.100501

10. Chen, G.-J., He, X.-Y., Wang, H.-Q., Nie, Y.-X., Zhai, C., Wen, Z.-N., & Mei, Y. (2026). Effect of geometric configuration on fluid flow characteristics and coal gasification performance in a shell gasifier. Applied Thermal Engineering, 298, 130943. https://doi.org/10.1016/j.applthermaleng.2026.130943

100. Zheng, H., Yang, M., Jiang, C.-F., & Liu, D.-J. (2021). Decomposition reaction of phosphate rock under the action of microwave plasma. Chinese Physics B, 30(4), 045201. https://doi.org/10.1088/1674-1056/abccb6

101. Zheng, Z., Li, J., Jin, Y., & Chen, M. (2020). Experimental determination and fitting of solid–liquid equilibria in the ternary system $BaO–P_2O_5–H_2O$ at 323.2 K. Journal of Chemical & Engineering Data, 65(1), 255–263. https://doi.org/10.1021/acs.jced.9b00977

102. Zhong, Y., Chen, Z., & Yang, X. (2022). Electrochemistry isolates elemental phosphorus from $Mg_3(PO_4)_2$. Journal of The Electrochemical Society, 169(10), 103503. https://doi.org/10.1149/1945-7111/ac9b98

103. Zhong, Y., Liu, G., & Yang, X. (2023). Isolating elemental phosphorus from sewage sludge ash by electrochemistry. Resources, Conservation and Recycling, 190, 106815. https://doi.org/10.1016/j.resconrec.2022.106815

104. Zhong, Y., Ma, Y., He, Y., & Yang, X. (2024). Extracting white phosphorus from $AlPO_4$ through molten salt processing. Electrochemistry, 92(4), 043015. https://doi.org/10.5796/electrochemistry.24-69001

105. Zhong, Y., & Yang, X. (2021). Dissolution behavior of solid $Ca_3(PO_4)_2$ in molten $CaCl_2$. Metallurgical and Materials Transactions B, 52(5), 3515–3523. https://doi.org/10.1007/s11663-021-02282-8

106. Zhu, R., Wang, Z., Luo, Y., Yang, E., Yang, S., Lin, Q., Pan, H., & Chen, Z. (2026). Removal of Mg^{2+} and Al^{3+} from high-concentration wet-process phosphoric acid by NH_4MgAlF_6 complexation-precipitation. Journal of Environmental Chemical Engineering, 14(1), 121094. https://doi.org/10.1016/j.jece.2026.121094

107. Zhu, Z., Tang, Y., Li, Z., He, D., & Yao, Y. (2022). Thermodynamics and kinetics analysis of phosphorus production by electric-furnace method. The Chinese Journal of Process Engineering, 22(7), 927–934. https://doi.org/10.12034/j.issn.1009-606X.221241

11. Chen, Z., Li, Y., & Xia, J. (2020). Silica, alkali carbonate and alkali rich metal ore as additive effect on the carbothermic reduction process of phosphorus ore. Silicon, 12(3), 613–620. https://doi.org/10.1007/s12633-019-00171-z

12. Dang, C., Wang, F., Zhao, Z., Liu, Z., & Guo, Y. (2020). Analysis of phosphorus material flow based on yellow phosphorus production process and countermeasures for phosphorus pollution reduction. Journal of Environmental Engineering Technology, 10(6), 1007–1011. https://doi.org/10.12153/j.issn.1674-991X.20200020

13. Deng, J., Zhang, K., He, D., Zhao, H., Hakkou, R., & Benzaazoua, M. (2020). Occurrence of sesquioxide in a mid-low grade collophane-sedimentary apatite ore from Guizhou, China. Minerals, 10(11), 1038. https://doi.org/10.3390/min10111038

14. Deng, X., Yin, S., Tang, S., Lv, L., & Zhang, T. (2026). Regulating co-crystalline phosphorus content in wet-process phosphoric acid via synergistic calcium sulfate crystallization and hydration. Chinese Journal of Chemical Engineering. Advance online publication. https://doi.org/10.1016/j.cjche.2026.02.004

15. Ding, W., Bao, S., Xin, C., Wang, Z., Zhang, H., & Kuang, B. (2025). Research progress on preparation and purification technology of wet-process phosphoric acid from middle-low-grade phosphorus ore. Chemical Industry and Engineering Progress, 44(4), 2274–2284. https://doi.org/10.16085/j.issn.1000-6613.2024-0567

16. Dli, M., Puchkov, A., Meshalkin, V., Abdeev, I., Saitov, R., & Abdeev, R. (2020). Energy and resource efficiency in apatite-nepheline ore waste processing using the digital twin approach. Energies, 13(21), 5829. https://doi.org/10.3390/en13215829

17. Dli, M., Puchkov, A., Vasiliev, A., Kirillova, E., Selyavskiy, Y., & Kulyasov, N. (2021). Intelligent control system architecture for phosphorus production from apatite-nepheline ore waste. Energies, 14(20), 6469. https://doi.org/10.3390/en14206469

18. Du, J., Zhai, C., Zhu, Y., Xie, D., & Mei, Y. (2021). Simulation study on heat energy recovery technology of furnace-process phosphoric acid process. CIESC Journal, 72(11), 5790–5799. https://doi.org/10.11949/0438-1157.20210817

19. Duan, Y., Li, R., Liu, Q., & Shen, Z. (2022). Elemental phosphorus for recent sustainable processes: Rules and strategies in preparation and applications. Green Chemistry, 24(9), 3475–3501. https://doi.org/10.1039/D2GC00727D

2. Abildayeva, A., Turgumbayeva, K., & Blumberga, D. (2021). Systematization of material flows of natural and secondary raw materials of phosphorus industry of the Republic of Kazakhstan. Environmental and Climate Technologies, 25(1), 894–906. https://doi.org/10.2478/rtuect-2021-0067

20. Fang, K., Xu, L., Yang, M., & Chen, Q. (2023). One-step wet-process phosphoric acid by-product $CaSO_4$ and its purification. Separation and Purification Technology, 309, 123048. https://doi.org/10.1016/j.seppur.2022.123048

21. Franke, E., Shalnev, S., Jahn, J., Pietschner, T., & Gräbner, M. (2025). Experimental investigations of thermochemical phosphorus release behavior from sewage sludge under inert and reducing conditions. Journal of Cleaner Production, 493, 144687. https://doi.org/10.1016/j.jclepro.2025.144687

22. Franke, E., Shalnev, S., Pietschner, T., & Gräbner, M. (2026). Phosphorus recovery from sewage sludge by thermochemical conversion: Separation from the gas phase and final product treatment. Chemical Engineering Journal Advances, 26, 101161. https://doi.org/10.1016/j.ceja.2026.101161

23. Gasik, M., Dashevskii, V., & Bizhanov, A. (2020). Ferroalloys: Theory and practice. Springer. https://doi.org/10.1007/978-3-030-57502-1

24. Geeson, M. B., & Cummins, C. C. (2020). Let's make white phosphorus obsolete. ACS Central Science, 6(6), 848–860. https://doi.org/10.1021/acscentsci.0c00332

25. Gilmour, R. (2019). Phosphorus. In Kirk-Othmer encyclopedia of chemical technology. Wiley. https://doi.org/10.1002/0471238961.1608151902182113.a01.pub3

26. Gong, X., Hu, C., Jin, Y., Liu, H., Bai, J., Niu, L., & Yang, L. (2024). Preparation of refined phosphoric acid with recycling of raffinate acid by the extraction of metal impurities.

Journal of Cleaner Production, 434, 140158. https://doi.org/10.1016/j.jclepro.2023.140158

27. Guo, J., Li, B., Zheng, G., Li, W., Xi, S., Yang, T., Zhang, Q., Du, J., Tao, C., & Liu, Z. (2025). Unraveling competitive cation-melamine complexation for efficient wet-process phosphoric acid purification via precipitation and gradient alkaline extraction. Chemical Engineering Journal, 524, 169357.https://doi.org/10.1016/j.cej.2025.169357

28. He, D., Zhang, Y., Fu, Y., Cao, Y., Tang, Y., Li, Z., & Yang, Q. (2025). Influence and mechanism on the preparation of pellets using phosphate ore powder. JOM, 77(9), 6637–6649. https://doi.org/10.1007/s11837-025-07559-w

29. He, X., & Huang, R. (2022). Effect of different carbon sources on vacuum carbothermal reduction of low-grade phosphorus ore. Chemical Industry & Chemical Engineering Quarterly, 28(1), 29–37. https://doi.org/10.2298/CICEQ210219013H

3. Ali, A. H. (2024). Sequential steps for purifying wet processed phosphoric acid for producing a high-tech grade and barium or ammonium phosphate salts. Russian Journal of Applied Chemistry, 97(2), 199–210. https://doi.org/10.1134/S107042722402006X

30. He, Y., & Yang, X. (2025). $MgCl_2$ enhances phosphate dissolution in molten $CaCl_2$. Metallurgical and Materials Transactions B, 56(1), 15–19. https://doi.org/10.1007/s11663-024-03404-8

31. Itkulova, S., Borangazieva, A., Ibraimova, Z., Polimbetova, G., & Boleubayev, E. (2021). Catalytic purification and ways for utilization of furnace gas of phosphorus production. Reports of the National Academy of Sciences of the Republic of Kazakhstan, 5(339), 136–143. https://doi.org/10.32014/2021.2518-1483.92

32. Jang, G. G., Thompson, J. A., Meyer, P. A., Zhang, P., Shen, Z., & Tsouris, C. (2024). Technoeconomic assessment of phosphoric acid and rare earth element recovery from phosphoric acid sludge. Sustainability, 16(16), 6984. https://doi.org/10.3390/su16166984

33. Ji, W., Xie, K., Yan, S., Huang, H., & Chen, H. (2020). A new method of recycling gallium from yellow phosphorus flue dust by vacuum thermal reduction process. Journal of Hazardous Materials, 400, 123234. https://doi.org/10.1016/j.jhazmat.2020.123234

34. Jiang, Z., Yu, H., Tian, Y., Yang, B., Xu, B., Kong, L., Liang, D., & Zhang, J. (2024). Investigation of arsenic removal from industrial yellow phosphorus through vacuum distillation: Thermodynamic and ab initio molecular dynamics. Separation and Purification Technology, 334, 126067. https://doi.org/10.1016/j.seppur.2023.126067

35. Jing, H., Hou, C., Wang, H., Yao, Y., & Liu, B. (2021). Slag activation in the carbothermic reduction of phosphorite with adding micronutrient-bearing cosolvents. JOM, 73(3), 941–950. https://doi.org/10.1007/s11837-020-04558-x

36. Jing, H., Shi, Y., Yuan, Y., Liu, B., Wang, Y., Guan, H., Gu, S., Wang, M., & Hou, C. (2024). Interface migration and alloying mechanism of Fe and P for ferrophosphorus alloy production during the carbothermic reduction of phosphorite. Journal of Solid State Chemistry, 338, 124907. https://doi.org/10.1016/j.jssc.2024.124907

37. Jing, H., Zhang, Y., Hu, L., Hou, C., He, H., Miao, J., Guan, H., Gu, S., & Wang, Y. (2025). From process optimization to resource recovery: The impact of K_2O and B_2O_3 fluxes on phosphorite reduction and slag fertilizer utilization. Chemical Engineering Journal, 525, 169857. https://doi.org/10.1016/j.cej.2025.169857

38. Jupp, A. R., Beijer, S., Narain, G. C., Schipper, W., & Slootweg, J. C. (2021). Phosphorus recovery and recycling—Closing the loop. Chemical Society Reviews, 50(1), 87–101. https://doi.org/10.1039/D0CS01150A

39. Kashiwakura, S., Okamoto, A., Kosai, S., Takizawa, M., & Yamasue, E. (2025). A promising silicothermic route for low-temperature, byproduct-free production of white phosphorus using silicon waste. ACS Sustainable Chemistry & Engineering, 13(50), 21537–21543. https://doi.org/10.1021/acssuschemeng.5c07921

4. Bahsaine, K., Mekhzoum, M. E. M., Benzeid, H., Qaiss, A. E. K., & Bouhfid, R. (2022). Recent progress in heavy metals extraction from phosphoric acid: A short review. Journal of Industrial and Engineering Chemistry, 115, 120–134. https://doi.org/10.1016/j.jiec.2022.08.029

40. Khajouei, M., Singh, B. K., Latifi, M., & Chaouki, J. (2025). Thermodynamic and experimental insights toward an eco-friendly phosphorus production. Cleaner Engineering and Technology, 29, 101092. https://doi.org/10.1016/j.clet.2025.101092

41. Khaless, K., Chanouri, H., Amal, S., Ouaattou, A., Mounir, E. M., Haddar, H., & Benhida, R. (2022). Wet process phosphoric acid purification using functionalized organic nanofiltration membrane. Separations, 9(4), 100. https://doi.org/10.3390/separations9040100

42. Kotze, A., Messina, D., Cryns, Y., Nagels, E., & Arnout, S. (2025). Thermochemical evaluation of elemental phosphorus recovery from sewage sludge. Journal of the Southern African Institute of Mining and Metallurgy, 125(9), 501–508. https://doi.org/10.17159/2411-9717/3556/2025

43. Li, B., Huang, R., Xie, R., Wu, Q., & Xu, A. (2022). A novel process for the direct utilization of copper slag and phosphate rock by compound modification and coreduction. Process Safety and Environmental Protection, 161, 629–639. https://doi.org/10.1016/j.psep.2022.03.079

44. Li, J., Zhao, C., Qu, G., Yuan, Y., Wu, F., Cheng, Y., Chen, B., Liu, S., & Ning, P. (2022). Electrochemically enhanced liquid-phase catalysis for simultaneous purification of phosphine, hydrogen sulfide and hydrogen cyanide: Interactions and synergistic

mechanisms. Journal of Environmental Chemical Engineering, 10(6), 108559. https://doi.org/10.1016/j.jece.2022.108559

45. Li, M., Ye, C., Li, S., Mei, Y., & Nie, Y. (2024). Current status and research progress of thermal reduction technology for producing yellow phosphorus from phosphate rock. Chemical Industry and Engineering Progress, 43(7), 3578–3592. https://doi.org/10.16085/j.issn.1000-6613.2023-2193

46. Li, P., Zhang, J., Luo, B., Li, Y., Ji, J., He, D., Tian, Q., & Chen, Y. (2021). Kinetics of carbothermal reduction process of different size phosphate rocks. Open Engineering, 11(1), 281–293. https://doi.org/10.1515/eng-2021-0025

47. Li, X., Huang, R., Wu, Q., Xie, S., & Li, J. (2021). Experimental approach for the characterization of low-grade phosphate ore performance in isothermal conditions. Journal of Sustainable Metallurgy, 7, 1736–1747. https://doi.org/10.1007/s40831-021-00451-2

48. Lidman Olsson, E. O., Glarborg, P., Dam-Johansen, K., & Wu, H. (2023). Review of phosphorus chemistry in the thermal conversion of biomass: Progress and perspectives. Energy & Fuels, 37(10), 6907–6998. https://doi.org/10.1021/acs.energyfuels.2c04048

49. Liu, G., Ma, Y., & Yang, X. (2024). Cleaner extraction of white phosphorus from phosphate rock through molten salt electrolysis. Journal of Cleaner Production, 434, 140374. https://doi.org/10.1016/j.jclepro.2023.140374

5. Baumgartner, S. J., Reynolds, Q. G., & Akdogan, G. (2024). Prediction of burden distribution and electrical resistance in submerged arc furnaces using discrete element method modelling. Journal of the Southern African Institute of Mining and Metallurgy, 124(3), 123–132. https://doi.org/10.17159/2411-9717/3042/2024

50. Liu, G., & Yang, X. (2025). Unraveling fluorapatite dissolution in molten $CaCl_2$ for sustainable phosphorus extraction. Journal of Environmental Chemical Engineering, 13(5), 117460. https://doi.org/10.1016/j.jece.2025.117460

51. Liu, X., Liu, X., & Zhang, Z. (2024). Application of yellow phosphorus slag in resource recovery and environmental remediation: A review. Journal of Environmental Management, 349, 119397. https://doi.org/10.1016/j.jenvman.2023.119397

52. Liu, Z., Yu, Q., Ma, W., Liu, J., & Tao, S. (2023). Experimental investigation on centrifugal granulation of molten yellow phosphorus slag. Chemical Engineering Research and Design, 197, 548–557. https://doi.org/10.1016/j.cherd.2023.08.006

53. Long, X., Deng, X., Lv, X., Wu, Q., Jin, H., Lu, F., Yang, J., & Huang, R. (2024). Study on the mechanism of vacuum carbothermal reduction of $Ca_3(PO_4)_2$ enhanced by SiO_2. Vacuum, 230, 113716. https://doi.org/10.1016/j.vacuum.2024.113716

54. Lu, Z., Bai, J., Kong, L., Li, H., Guo, Z., Bai, Z., & Li, W. (2024). Effect of SiO_2/CaO on the viscosity and structure of yellow phosphorus slag in the electric furnace. Fuel, 358, 130214. https://doi.org/10.1016/j.fuel.2023.130214

55. Lu, Z., Lu, H., Huang, L., Kong, L., Li, H., Bai, J., Guo, Z., Bai, Z., & Li, W. (2023). Effect of P_2O_5 on the viscosity of yellow phosphorus slag in electric furnace at high temperatures. Fuel, 333, 126374. https://doi.org/10.1016/j.fuel.2022.126374

56. Lu, Z., Wang, Y., Bai, J., Kong, L., Li, H., Guo, Z., Bai, Z., & Li, W. (2025). Effect of cation affinity properties of phosphorus on slag structure and phase separation in phosphorus ore smelting slags. Journal of Non-Crystalline Solids, 664, 123616. https://doi.org/10.1016/j.jnoncrysol.2025.123616

57. Luckins, E. K., Oliver, J. M., Please, C. P., Sloman, B. M., Valderhaug, A. M., & Van Gorder, R. A. (2022). Modelling alternating current effects in a submerged arc furnace. IMA Journal of Applied Mathematics, 87(3), 492–520. https://doi.org/10.1093/imamat/hxac012

58. Luo, B., Li, P., Li, Y., He, P., Ji, J., He, D., & Tian, Q. (2020). Optimization of medium–low-grade phosphorus rock carbothermal reduction process by response surface methodology. Green Processing and Synthesis, 9(1), 349–358. https://doi.org/10.1515/gps-2020-0035

59. Luo, B., Li, P., Li, Y., Ji, J., He, D., Tian, Q., & Chen, Y. (2021). Feasibility of fly ash as fluxing agent in mid- and low-grade phosphate rock carbothermal reduction and its reaction kinetics. Green Processing and Synthesis, 10(1), 157–168. https://doi.org/10.1515/gps-2021-0008

6. Becker, P. (1989). Phosphates and phosphoric acid: Raw materials, technology, and economics of the wet process (2nd ed., rev. and expanded). Marcel Dekker.

60. Ma, Y., & Yang, X. (2024). Electrochemical reduction behavior of PO_4^{3-} ions in molten $CaCl_2$. Electrochimica Acta, 507, 145071. https://doi.org/10.1016/j.electacta.2024.145071

61. Melville, J. F., Licini, A. J., & Surendranath, Y. (2023). Electrolytic synthesis of white phosphorus is promoted in oxide-deficient molten salts. ACS Central Science, 9(3), 373–380. https://doi.org/10.1021/acscentsci.2c01336

62. Meshalkin, V. P., Bobkov, V. I., Dli, M. I., Fedulov, A. S., & Shinkevich, A. I. (2021). Computer-assisted decision-making system of optimal control over the energy and resource efficiency of a chemical energotechnological system for processing apatite–nepheline ore wastes. Theoretical Foundations of Chemical Engineering, 55(1), 62–69. https://doi.org/10.1134/S0040579521010103

63. Nezamaev, S., Dli, M., Orekhov, V., & Bobkov, V. (2025). Technological substantiation of the raw phosphorite processing ore based on its chemical and granulometric

composition. AIP Conference Proceedings, 3347(1), 020063. https://doi.org/10.1063/5.0293123

64. Pak, H.-T., Ri, S.-H., Pak, S.-O., Choe, S.-J., & Ri, O.-I. (2026). Anthracite briquettes prepared with phosphate compounds and silicon as carbonaceous reducing agent alternative to coke for yellow phosphorus production. Russian Journal of General Chemistry, 96(5), 116. https://doi.org/10.1134/S1070363225606805

65. Pan, F., Mei, Y., Yang, Y., Xie, D., & Nie, Y. (2026). Efficient absorption of COS and CS_2 in methanol for yellow phosphorus tail gas purification: Thermodynamic, kinetic and molecular insights. Chemical Engineering Journal, 527, 171713. https://doi.org/10.1016/j.cej.2025.171713

66. Ridlo, F. 'A., Rhamdhani, M. A., Pownceby, M. I., Nababan, D. C., Hakim, B., Erlangga, P. Y., Fauth, S. S., Ritonga, G. F., Hendrawan, Y., Hidayat, T., & Zulhan, Z. (2026). Phosphorus removal from monazite concentrates via hydrogen plasma smelting. Metallurgical and Materials Transactions B, 57(4), 2356–2373. https://doi.org/10.1007/s11663-026-03985-6

67. Smailov, B., Ismailov, B., Zakirov, B., Turakulov, B., Tursynbay, L., & Aimenova, Z. (2024). Study and mechanism of formation of phosphorus production waste in Kazakhstan. Green Processing and Synthesis, 13(1), 20240023. https://doi.org/10.1515/gps-2024-0023

68. Tang, S., Li, Y., Xu, P., Zhang, T., Lv, L., Tang, W., Zou, Z., Wang, Y., & Zhou, K. (2026). Occurrence and migration of metallic impurities in a novel clean gypsum route for phosphoric acid production. Journal of Environmental Chemical Engineering, 14(5), 124119. https://doi.org/10.1016/j.jece.2026.124119

69. Tang, X., Li, B., Yu, Y., Wang, S., Xu, J., & Liu, Z. (2025). Analysis and optimization about heat and mass transfer in silicon submerged arc furnace. Applied Thermal Engineering, 281, 128737. https://doi.org/10.1016/j.applthermaleng.2025.128737

7. Bertau, M., Wellmer, F.-W., Scholz, R. W., Mew, M., Zenk, L., Aubel, I., Fröhlich, P., Raddant, M., & Steiner, G. (2025). The future of phosphoric acid production—Why we have to leave trodden paths. ChemSusChem, 18(3), e202401155. https://doi.org/10.1002/cssc.202401155

70. Tang, X., Yu, Y., Rong, W., Li, B., & Liu, Z. (2026). Study on eddy current losses in a full-scale large AC submerged arc furnace with all components. Metallurgical and Materials Transactions B. Advance online publication. https://doi.org/10.1007/s11663-026-04216-8

71. Tesfahunegn, Y. A., Magnusson, T., Tangstad, M., & Saevarsdottir, G. (2021). The effect of electrode movements on electrical characteristics of a submerged arc furnace. JOM, 73(10), 2963–2972. https://doi.org/10.1007/s11837-021-04818-4

72. Tesfahunegn, Y. A., Magnússon, Þ., Tangstad, M., & Sævarsdóttir, G. A. (2020). Comparative study of AC and DC solvers based on current and power distributions in a submerged arc furnace. Metallurgical and Materials Transactions B, 51(2), 510–518. https://doi.org/10.1007/s11663-020-01794-z

73. Tian, Z., Zhang, B., Yue, J., & Wang, Q. (2025). Feasibility analysis and mechanism study of different sulfate waste residues for carbothermal reduction of phosphorite in a fluidized bed. Journal of Industrial and Engineering Chemistry, 150, 668–683. https://doi.org/10.1016/j.jiec.2025.03.030

74. Volnenko, A. A., Zhumadullayev, D. K., Korganbayev, B. N., Abzhapbarov, A. A., & Issayeva, A. N. (2023). Development and calculation of an apparatus with a ring tubular filling for modernization of a cooling-hydration tower in thermal phosphoric acid production. International Review of Mechanical Engineering, 17(1), 14–21. https://doi.org/10.15866/ireme.v17i1.23387

75. Wang, J., Jiang, Y., Tian, Z., Li, J., Jin, Y., Chen, J., & Wang, Y. (2025). Highly permeable acid-stable poly(sulfonamide-urea) nanofiltration membrane for purifying phosphoric acid. Separation and Purification Technology, 362, 131662. https://doi.org/10.1016/j.seppur.2025.131662

76. Wang, X., An, Y., Liu, H., & Tian, M. (2023). Carbon footprint analysis of yellow phosphorus products based on LCA. Inorganic Chemicals Industry, 55(12), 36–42. https://doi.org/10.19964/j.issn.1006-4990.2023-0222

77. Wieser, D., Ortner, B., Prieler, R., Mally, V., & Hochenauer, C. (2026). Development of a numerically inexpensive 3D CFD model of slag reduction in a submerged arc furnace for phosphorus recovery from sewage sludge. Processes, 14(2), 289. https://doi.org/10.3390/pr14020289

78. Wingate, E., Prasad, R., & Liu, Y. (2023). Phosphorus—A circular journey from the ground to the recycling line. Mining, Metallurgy & Exploration, 40, 1469–1485. https://doi.org/10.1007/s42461-023-00839-6

79. Wu, F., Zhao, C., Qu, G., Liu, S., Ren, Y., Chen, B., Li, J., & Liu, L. (2022). A critical review of the typical by-product clean ecology links in the Chinese phosphorus chemical industry in China: Production technologies, fates and future directions. Journal of Environmental Chemical Engineering, 10(2), 106685. https://doi.org/10.1016/j.jece.2021.106685

8. Borangazieva, A. K., Boleubayev, Y. A., Ibraimova, Z. U., Itkulova, S. S., & Polimbetova, G. S. (2023). Catalytic oxidation of phosphine by aqueous copper–ammonia complexes. Catalysts, 13(2), 271. https://doi.org/10.3390/catal13020271

80. Wu, P., Lü, L., Tang, S., Liu, C., Yue, H., Jiang, W., & Liang, B. (2020). The fouling properties of SiO_2–CaO–P_2O_5 system in high-temperature rotary kiln phosphoric acid process. Chinese Journal of Chemical Engineering, 28(7), 1824–1831. https://doi.org/10.1016/j.cjche.2020.01.005

81. Wu, Q., Li, J., Lv, X., Xv, B., Chen, C., & Huang, R. (2021). Reaction mechanism of low-grade phosphate ore during vacuum carbothermal reduction. Metallurgical and Materials Transactions B, 52(3), 1484–1494. https://doi.org/10.1007/s11663-021-02117-6

82. Xie, S., Yang, J., Huang, R., Lv, X., Li, X., & He, X. (2024). A novel process for the separation and recovery of phosphorus and rare earth elements from associated rare earth phosphate ores. Separation and Purification Technology, 340, 126687. https://doi.org/10.1016/j.seppur.2024.126687

83. Xu, C., Liu, Y., Zhang, M., Peng, X., Zheng, J., Wang, H., Meng, Z., Zhu, G., Cui, Y., Jiang, X., & Sun, G. (2026). Cyclic solvent extraction with OIDMDPPA and oxalate stripping to recover purified H_3PO_4, $Al(OH)_3$ and battery grade $FeC_2O_4 \cdot 2H_2O$ from wet-process phosphoric acid. Hydrometallurgy, 241, 106663. https://doi.org/10.1016/j.hydromet.2026.106663

84. Xu, C., Zhang, M., Liu, Y., Peng, X., Li, T., Li, W., Meng, Z., Zhu, G., Cui, Y., Jiang, X., & Sun, G. (2025). Construction of multidentate phosphonic acid ligand for targeted multi-metal extraction toward purification of wet-process phosphoric acid: Mechanistic insights into Fe^{3+} chelation. Chemical Engineering Journal, 521, 166957. https://doi.org/10.1016/j.cej.2025.166957

85. Xu, S., He, R., Dong, C., Sun, N., Zhao, S., He, H., Yu, H., Zhang, Y.-B., & He, T. (2022). Acid stable layer-by-layer nanofiltration membranes for phosphoric acid purification. Journal of Membrane Science, 644, 120090. https://doi.org/10.1016/j.memsci.2021.120090

86. Yang, B., Ge, Z., Zhang, X., & Guo, L. (2025). Kinetic analysis on carbothermal reduction process of phosphorite based on the isoconversional methods. Chemical Engineering Science, 317, 122090. https://doi.org/10.1016/j.ces.2025.122090

87. Yang, X., & Nohira, T. (2020). A new concept for producing white phosphorus: Electrolysis of dissolved phosphate in molten chloride. ACS Sustainable Chemistry & Engineering, 8(36), 13784–13792. https://doi.org/10.1021/acssuschemeng.0c04796

88. Yang, Y., Nie, Y., Pan, F., Wen, Z., Xie, D., Zhu, Y., & Mei, Y. (2025). Novel technology for eliminating phosphine from yellow phosphorus tail gas through the rectisol process. Separation and Purification Technology, 372, 133443. https://doi.org/10.1016/j.seppur.2025.133443

89. Yang, Y., Nie, Y., Pan, F., Wen, Z., Xie, D., Zhu, Y., & Mei, Y. (2026). Rectisol purification of PH_3, H_2S, and CO_2 from yellow phosphorus tail gas: Mechanistic insights and resource recovery. Journal of Environmental Chemical Engineering, 14(1), 121122. https://doi.org/10.1016/j.jece.2026.121122

9. Cen, Y., Zhang, F., Jiang, X., Lei, Z., & Chen, Z. (2026). Study on oxidation-roasting performance and consolidation mechanism of phosphate ore pellets. Minerals, 16(5), 433. https://doi.org/10.3390/min16050433

90. Yao, Y., Jing, H., Yin, Y., Qi, S., Wang, Y., & Hou, C. (2024). Research status and suggestions of yellow phosphorus production technology by thermal processing under peak carbon dioxide emission and carbon neutrality. Chemical Industry and Engineering Progress, 43(4), 2104–2116. https://doi.org/10.16085/j.issn.1000-6613.2023-0560

91. Yu, H., Lu, X., Miki, T., Matsubae, K., Sasaki, Y., & Nagasaka, T. (2022). Sustainable phosphorus supply by phosphorus recovery from steelmaking slag: A critical review. Resources, Conservation and Recycling, 180, 106203. https://doi.org/10.1016/j.resconrec.2022.106203

92. Yu, H., Miki, T., Sasaki, Y., & Nagasaka, T. (2022). Simultaneous reduction of P_2O_5 and FeO from CaO–SiO_2–FeO–P_2O_5 synthesized slag by carbothermic reduction. Metallurgical and Materials Transactions B, 53(3), 1806–1815. https://doi.org/10.1007/s11663-022-02488-4

93. Yu, H., Yoshida, R., Ohtake, H., Sasaki, Y., & Nagasaka, T. (2024). White phosphorus production by a carbothermic reduction of upcycled crude phosphoric acid. Resources, Conservation and Recycling, 211, 107868. https://doi.org/10.1016/j.resconrec.2024.107868

94. Yu, L., Zhou, J., Dong, J., Wang, S., Yang, X., Jia, S., Wang, J., Tang, W., Hu, G., & Gong, J. (2026). Trace impurity migration and enrichment mechanism on the highly efficient purification of electronic-grade phosphoric acid through melt crystallization. Separation and Purification Technology, 390, 136999. https://doi.org/10.1016/j.seppur.2026.136999

95. Yu, X., Wang, L., Hu, W., Wang, M., & Zhu, B. (2026). Low-carbon transition of phosphorus chemical industrial parks: A global systematic review. Global Environmental Change, 96, 103080. https://doi.org/10.1016/j.gloenvcha.2025.103080

96. Yu, Y., Li, B., Liu, Z., Qi, F., Liu, C., Rong, W., & Kuang, S. (2023). Analysis of electrical energy consumption in a novel direct current submerged arc furnace for ferrochrome production. Metallurgical and Materials Transactions B, 54(5), 2370–2382. https://doi.org/10.1007/s11663-023-02838-w

97. Yu, Y., & Yang, X. (2024). Dissolution of solid $FePO_4$ in molten $CaCl_2$. Metallurgical and Materials Transactions B, 55(2), 758–771. https://doi.org/10.1007/s11663-023-02988-x

98. Zhao, C., Cheng, Y., Qu, G., Yuan, Y., Wu, F., Liu, Y., Liu, S., Li, J., & Ning, P. (2023). High-performance liquid-phase catalytic purification of phosphine in tail gas using Pd(II)/Cu(II) composite. Chinese Journal of Chemical Engineering, 57(5), 98–108. https://doi.org/10.1016/j.cjche.2022.08.017

99. Zheng, G., Cao, R., Li, Y., Xia, J., & Chen, Z. (2020). The additive effect of K_2CO_3–$NiSO_4$ on the carbothermal reduction process of phosphate rock and SiO_2. Silicon, 12, 1985–1994. https://doi.org/10.1007/s12633-019-00311-5

APPENDICES

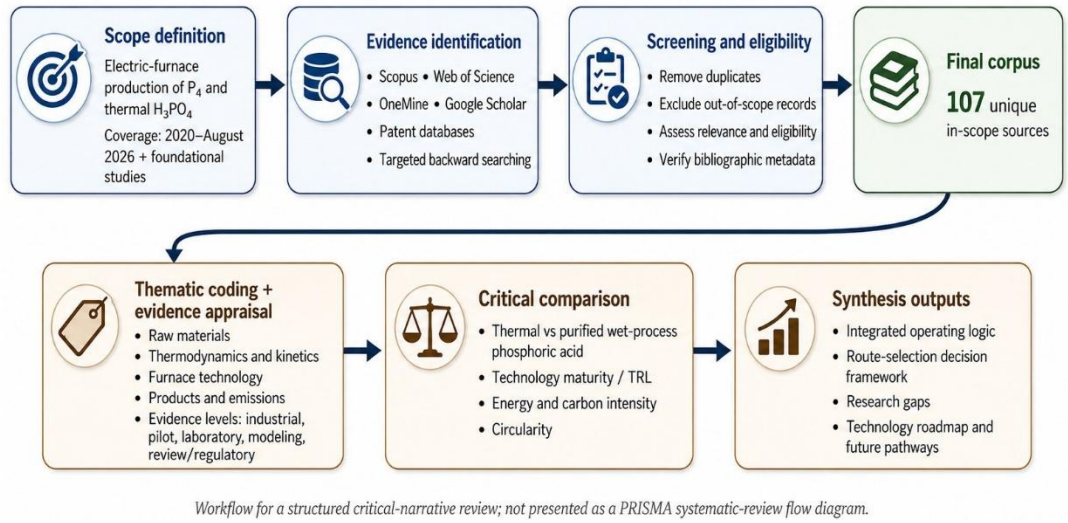
APPENDIX A

Highlights

- Electric-furnace phosphorus remains technically robust but structurally energy- and carbon-intensive.
- The historical purity advantage is narrowing as wet-process acid purification becomes more capable.
- Slag chemistry, burden permeability, electrical behavior, and gas removal must be optimized as one coupled system.
- Future competitiveness depends on low-carbon electricity, resource recovery, and alternative phosphorus-production routes.

Figure 1

Graphical abstract



Source: Prepared by the authors.

APPENDIX B

NOMENCLATURE

TABLE 1

Selected symbols and abbreviations

Symbol/abbreviation	Meaning
AI	Artificial intelligence
CAPEX	Capital expenditure
CFD	Computational fluid dynamics
CO	Carbon monoxide
CO_2	Carbon dioxide
H_3PO_4	Phosphoric acid
LCA	Life cycle assessment
OPEX	Operating expenditure
P_2O_5	Phosphorus pentoxide equivalent/phosphate expression
P_4	Elemental phosphorus (tetraphosphorus)
PH_3	Phosphine
PRISMA	Preferred Reporting Items for Systematic Reviews and Meta-Analyses
REE / REEs	Rare earth element / rare earth elements
TRL	Technology readiness level

Note. Compiled by the author for this review.